Joint Centre for Mesoscale Meteorology, Reading, UK

A Case Study of High Resolution Fog Forecasts with the New Dynamics

P. Clark

Internal Report No. 123
NWP Technical Report No. 337

November 2000

Met Office Joint Centre for Mesoscale Meteorology Department of Meteorology
University of Reading PO Box 243 Reading RG6 6BB United Kingdom
Tel: +44 (0)118 931 8425 Fax: +44 (0)118 931 8791
www.metoffice.com

Designed and produced by the Met Office © Crown copyright 2001 01/0240 The Met Office logo is a registered trademark.

A Case Study of High Resolution Fog Forecasts with the New Dynamics

Peter Clark
November, 2000

Abstract

This Report details initial experience running the New Dynamics (ND) at high horizontal resolution (4 km and 2 km) with one case of widespread fog. Results are compared with results at the current operational resolution, using both the ND and the current, hydrostatic UM. The assessment is intended to be purely meteorological. Tuning or even re-formulation of certain parametrization schemes may, in future, prove necessary to run well at higher resolution. This Report makes no attempt to perform such tuning, but is merely intended to indicate whether the model provides sufficient encouragement to form the basis of future work.

Model performance is complex and of mixed quality. The ND at operational resolution performs generally better objectively and subjectively than the hydrostatic UM with the same physics. Sensitivity to vertical resolution is not strong at operational (12 km) resolution. The ND has been successfully run at 4 km and 2 km resolution. Both produce very good short (6-12h) forecasts compared with the 12 km model, though the benefit of going from 4 to 2 km is not clear. A 12 h forecast covering the whole UK at 4 km would be a practical proposition, given the additional computing power required to add this to our current operational suite. The higher resolution runs, however, exhibit problems with excessive deepening, thickening and lifting of fog as time progresses, and eventually perform worse than lower resolution runs. The reason for this behaviour is unknown, but possible explanations include inaccurate initial conditions or excessive entrainment through the fog top in the boundary layer scheme.

Contents

1 **INTRODUCTION** 1

2 **THE CASE** 1

3 **MODEL SIMULATIONS** 6

3.1 UM REFERENCE RUNS 6
3.2 NEW DYNAMICS CONFIGURATION 7
3.3 MODEL TECHNICAL DETAILS, PROBLEMS AND SOLUTIONS 10
3.4 VERIFICATION METHODS 11
3.5 FOG RESULTS 12
3.6 MODEL WINDS 17
3.7 CROSS SECTIONS 22
3.8 DISCUSSION 25

4 **CONCLUSIONS AND RECOMMENDATIONS** 26

5 **REFERENCES** 27

1 Introduction

Radiation fog presents a particular challenge to numerical forecast systems. Sufficiently high vertical resolution near the surface is required to begin to represent the boundary layer and radiation processes involved. This can, to some extent, be provided by 1D treatments such as the Site Specific Forecast Model (Clark et al, 1997). However, it is a matter of common experience that considerable small scale horizontal variability can occur induced by variations in surface elevation, surface characteristics such as vegetation and moisture, and more transient features such as mid and upper level cloud. High resolution 3D models are thus a potential way forward. The advent of the non-hydrostatic 'New Dynamics' (ND) in the Unified Model (UM) brings with it the scientific possibility of implementing NWP systems at resolutions high enough to require non-hydrostatic dynamics for some phenomena. While it is unlikely that non-hydrostatic dynamics are of particular importance to fog formation, it is likely that fog forecasts may benefit particularly from improved horizontal resolution.

This report details initial experience running the ND at high horizontal resolution with one case of widespread fog. Results are compared with results at the current operational resolution, using both the ND and the current, hydrostatic UM. Though some objective verification is performed, no attempt has been made to assess against the NWP index or similar, partly because not all the diagnostics needed are available, but mainly because such a comparison is regarded as fruitless based, as it would be, on a single case with unrealistic assimilation conditions. The assessment is intended to be purely meteorological. Tuning or even re-formulation of certain parametrization schemes may, in future, prove necessary to run well at higher resolution. This Report makes no attempt to perform such tuning, but is merely intended to indicate whether the model provides sufficient encouragement to form the basis of future work.

2 The Case

A case, 21-22/01/1999, was chosen which met the following criteria:

- Widespread and reasonably long-lasting radiation fog visible on satellite imagery and observed at a number of synoptic stations.
- Some evidence of orographic blocking of fog – clear regions at some hill tops.
- A reasonably accurate operational forecast in terms of synoptic conditions and at least a tendency to form fog.

An indication of the extent of fog and low cloud is given in Fig. 1, which shows AVHRR satellite imagery, primarily the 'Fog' product, which may, of course, also indicate low cloud not in contact with the surface. Visible Meteosat imagery, where available, shows much the same pattern, with less detail, and, of course, is not available at night. Fig. 1 shows very low cloud with a distribution, confined largely to the Severn, Avon and Thames valleys plus much of Somerset in central and southern England, with, perhaps, more scattered 'fog' around Cambridgeshire and Bedfordshire, extending into Northamptonshire. The constancy of the 'fog' distribution is striking, but some trends do occur. As time progresses, a tongue of fog extends into the Bristol Channel and south Wales, and there is eventually some development over central Norfolk and into Lincolnshire though, interestingly, most of the lowest ground around the Fens remains free. For most of the time, the major ranges of hills, such as the Cotswolds, Chilterns, Marlborough Downs, Mendips and the West Midlands remain clear of fog and clearly delineated by the valley fog. There is some hint in the later visible image of some formation over the Cotswolds. Some of the narrower river valleys in SW England and Wales also show some evidence of fog.

Fig. 2 shows observed visibility from synoptic stations at 18Z and 21Z on the 21st and 00Z, 03Z, 06Z and 09Z. The area and orography shown is from the 2 km resolution model to be discussed below. These observations illustrate many of the problems of fog forecasting and verification. In comparison with the structure shown in Fig. 1 they are very sparse. In the main area of fog, they conform to the idea that the fog is roughly confined to regions with an altitude below about 100m asl, the top perhaps lifting later in the period (i.e. increasingly so after 06Z). Where clusters of observations do occur, they can show very different values as a result of altitudes differing by a few tens of meters. A quality control system which compared adjacent sites might well reject such data if no account were taken of altitude. Even if not rejected, it is likely that such data would not have the desired impact in a data assimilation system using spatially homogeneous error covariances. Such errors have, indeed, been shown to occur in similar circumstances, where the heterogeneous fog distribution resulted in large temperature gradients.

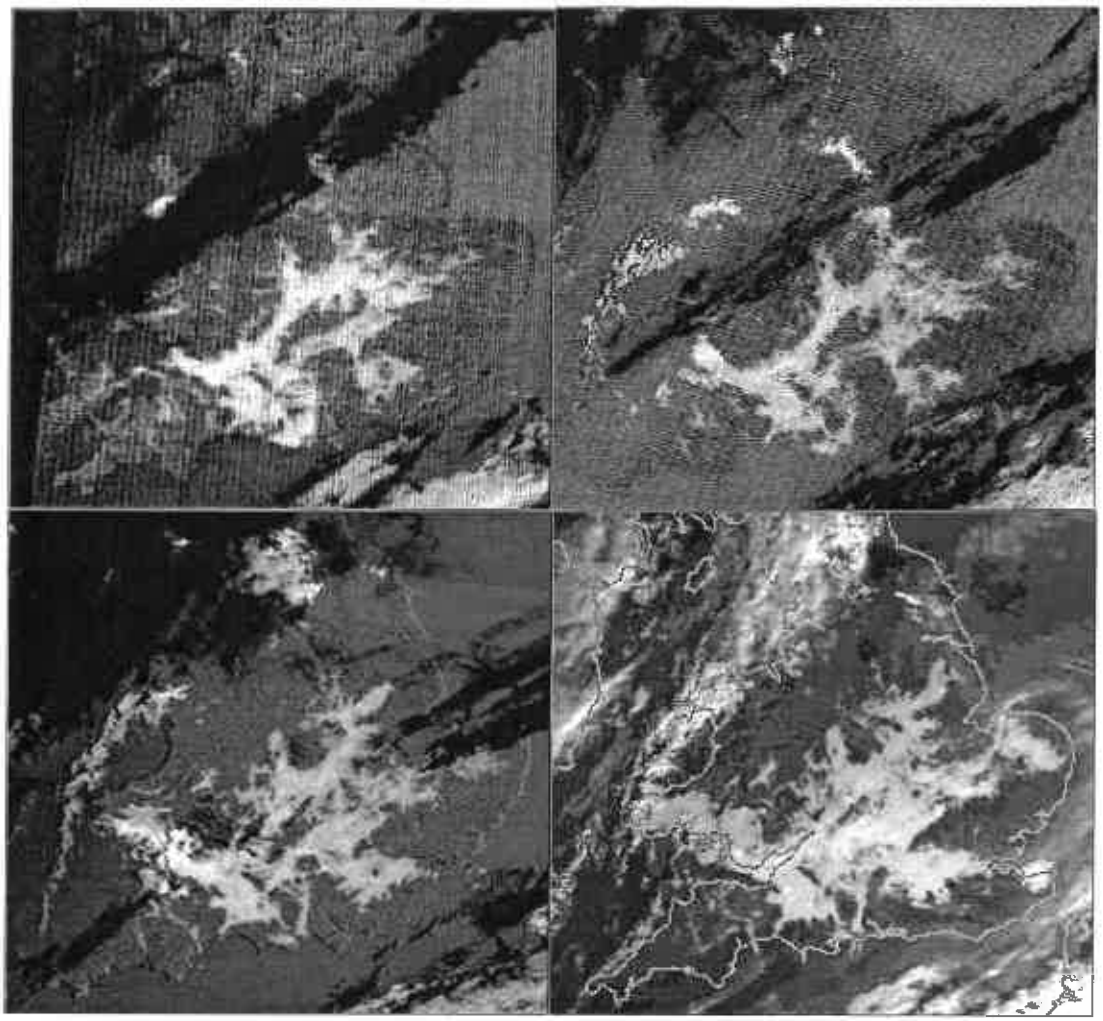

Figure 1 Fog Images 0255Z (Top Left) 0555Z (Top Right) 0740Z (Bottom Left) and Visible Image at 0920Z, all from AVHRR Passes on 22/1/99

For the most part, the satellite data of Fig. 1 and the surface observations of Fig. 2 are consistent. However, it should be remembered that the satellite data shows low cloud, which may, or may not, have lifted off the surface, while the surface observations may show small, and/or shallow patches which are not sufficient to show up on the satellite image. This is especially true of manual visibility observations, which report the minimum horizontal visual range in any direction, so may pick up a small patch of fog that is not even present at the observing site.

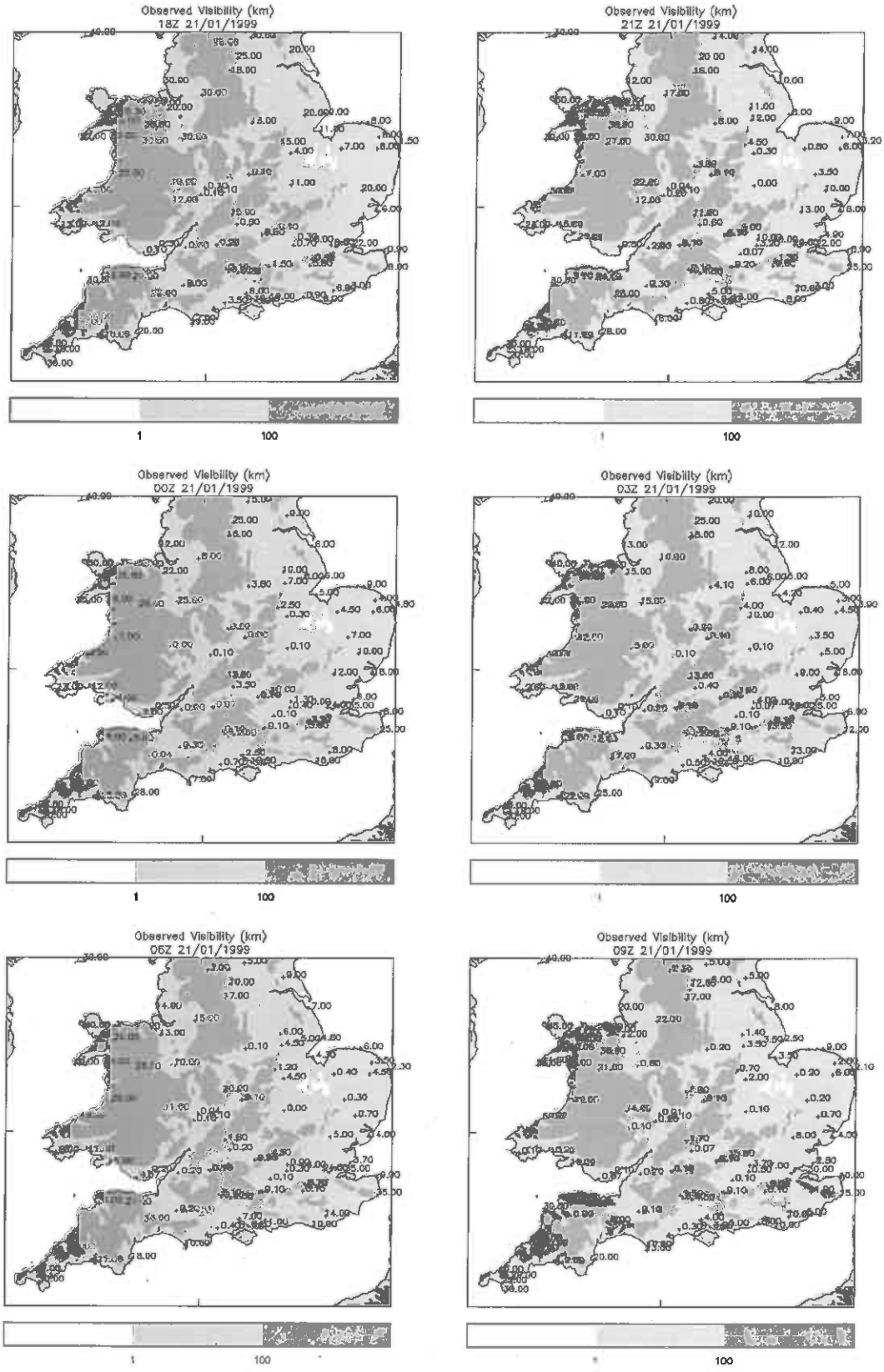

Figure 2 Visibility in km from Synoptic Stations shown on 100m contour from 2 km resolution model orography.

The observed Pressure at Mean Sea Level (PMSL) is illustrated in Fig. 3 for 00Z on the 22nd. This confirms that the pressure gradient was extremely slack, with a variation of only about 2-3 hPa over the whole of England south of the Humber and Wales. The highest pressure was around Devon and Somerset, though there is a great deal of small scale variability, some of which my be contributed to by artefacts of the reduction of pressure to MSL. Lowest pressures are found along the SE coast and the Norfolk/Lincolnshire/Yorkshire coast.

Fig. 4 shows observed 10 m wind at 00Z, 03Z, 06Z and 09Z on the 22nd, plotted as vectors pointing with the wind. As expected, wind speeds are very low, often calm. In particular, the majority of lowland, foggy stations show calm or very close to calm. Such calms should be treated with caution, as the minimum measurable speed depends on the type of anemometer, and can be more than 1 m/s for an older 'Monroe' model, and at least 0.5 m/s for more modern instruments. Where directions have been reported at calm sites, they tend, as one might expect, to vary substantially with time. Given this uncertainty, where significant winds are observed, they show substantial consistency with time. To the NW, the wind appears fairly consistent with the pressure gradient, though, as expected, somewhat backed. To the south there is also some consistency with the pressure gradient, which would give a geostrophic wind running roughly parallel to the coast from the east. However, there is substantial spatial variability, and the orientation of the wind directions would be quite consistent with a significant land breeze component.

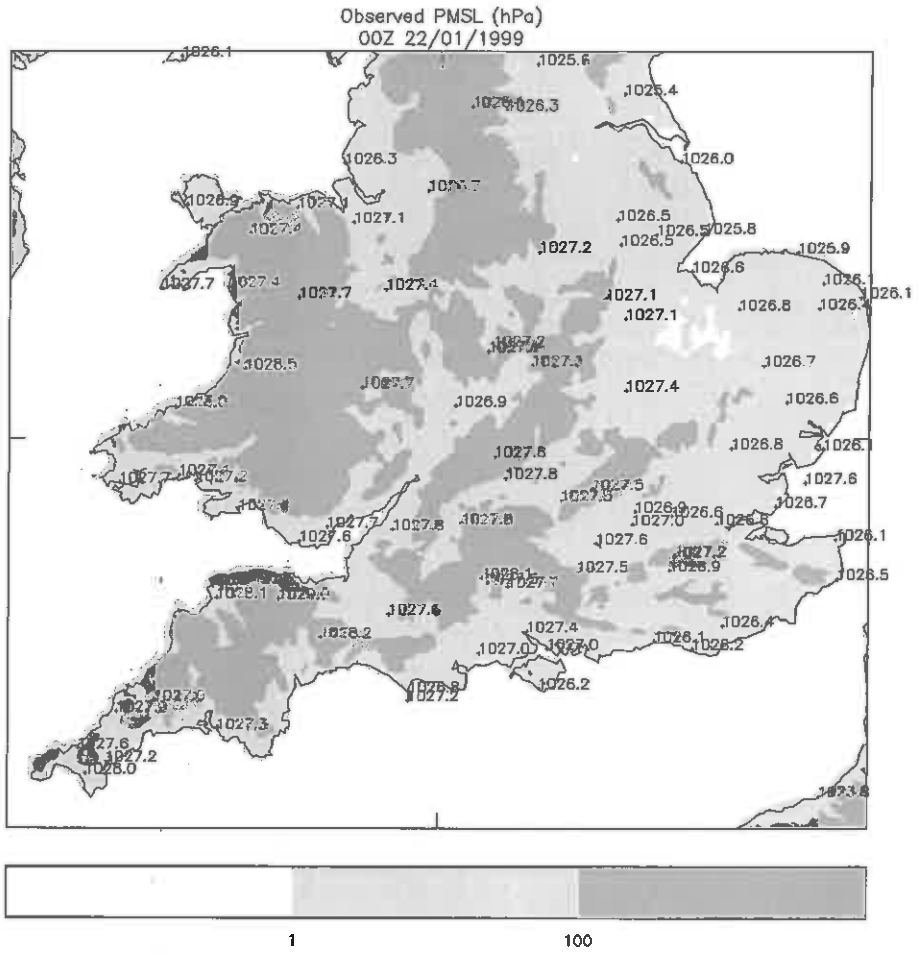

Figure 3 Observed Pressure at Mean Sea Level at 00Z, 22/1/99 from synoptic stations

Some individual stations show interesting behaviour. The elevated site (Little Rissington) near the centre of the Cotswolds shows a relatively strong wind at 2-4 m/s which steadily veers throughout the night, which may be associated with the veering of down slope winds by the Coriolis force, though the wind speed dies away during the morning. Manchester shows a fairly steady southerly flow; in fact, the flow changes from westerly to southerly at around 23Z on the 21st, suggesting that the flow has become blocked by the southern Pennines. There is no suggestion that the flow becomes unblocked until the afternoon.

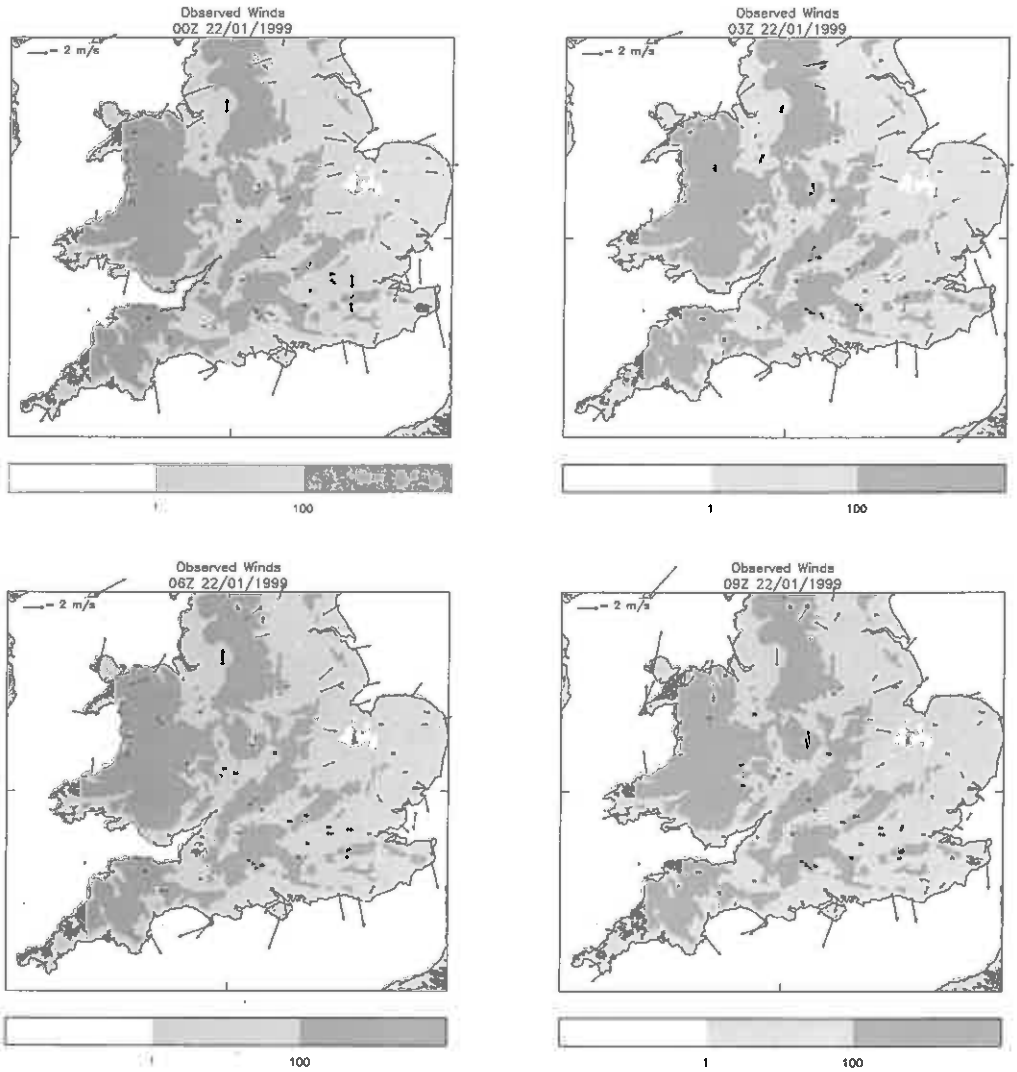

Figure 4 Observed 10 m winds from synoptic stations

Temperatures during the night show the anticipated general cooling; no obvious patterns emerge in their distribution except that the lowland, generally foggy regions fall below zero (typically to -2 or -3 °C), while the more exposed sites managed to stay marginally above. The fact that the fog was freezing may have some implications for the model simulations to follow.

3 Model Simulations

3.1 UM reference runs

The case was chosen, in part, because the then-operational mesoscale model produced a reasonable, though by no means outstanding, forecast. Widespread fog was, indeed forecast over much of central and southern England, but the spatial distribution was not very good. The ND code only has one set of physics, essentially HADAM4a. Amongst other things, this has a markedly different boundary layer scheme (the '6A' scheme, with non-local treatment of the unstable boundary layer and revised stable stability functions) and a different radiation scheme, both of which, of course, are central to radiation fog formation. To enable a reasonably valid comparison with the ND, the UM has been rerun with physics parametrizations which, it is believed, are as close as possible to the ND physics. Unfortunately, it has proven impossible to locate definitive documentation as to the physics included in the ND, so, short of going through the code line by line, correspondence cannot be verified and so guaranteed. As an aside, it is the opinion of this author that such a level of documentation effectively invalidates any comparison between the ND and the current quasi-hydrostatic dynamics where diabatic processes have any significant role. The overall performance can, of course, be assessed, but, should discrepancies occur, it will be very difficult to identify whether the cause is a change in physics or dynamics.

Forecasts were run from the 12Z analysis on the 21st. This was chosen for a number of reasons. Although there was some fog present at this time, it represents roughly a minimum, so the forecast was not too dominated by pre-existing fog, and actually simulated the formation process. The 12Z run is probably the latest run from which forecasts for early morning fog would be made in many circumstances (though short TAFs would be able to use later data). In practice, running higher resolution forecasts might be run over a shorter period, but only with an associated analysis. It is likely that some early artefacts would arise from reconfiguring a lower resolution analysis onto high resolution orography. Whilst these might persist, we hope to avoid the worst effects by reconfiguring a less stable, daytime boundary layer and assessing the forecast after some time has elapsed. Given the light winds, boundary issues are not too much concern in this case.

With the ND equivalent physics, the character of the fog forecast changes markedly. Fog extent is markedly and excessively increased. Fig 5. Shows the screen level cloud fraction at 06Z on the 22nd from the two runs. As a matter of interest, the 'ND Physics' run also shows some sign of numerical artefacts to the south of France.

These differences could be the result of a number of factors. The most important are probably the boundary layer formulation and the soil temperature and soil moisture. The boundary layer formulation used in the ND and HADAM4a physics uses the 'sharpest' stable stability functions which tend to lead to shallower stable boundary layer depths and thicker fog. Because MOSES was not operational at the time, a change to the surface and soil scheme was also necessary, which involved using climatological soil temperature and soil moisture. The soil moisture content may not be so important, as by January the soil was probably close to saturation anyway, but the soil temperatures may well have had a significant impact, especially as UM climatology tends to be a little cold over the UK. No facilities are available to transfer soil data from the UM to the ND so the ND must be run with climatology – therefore, running the UM control with climatology is appropriate.

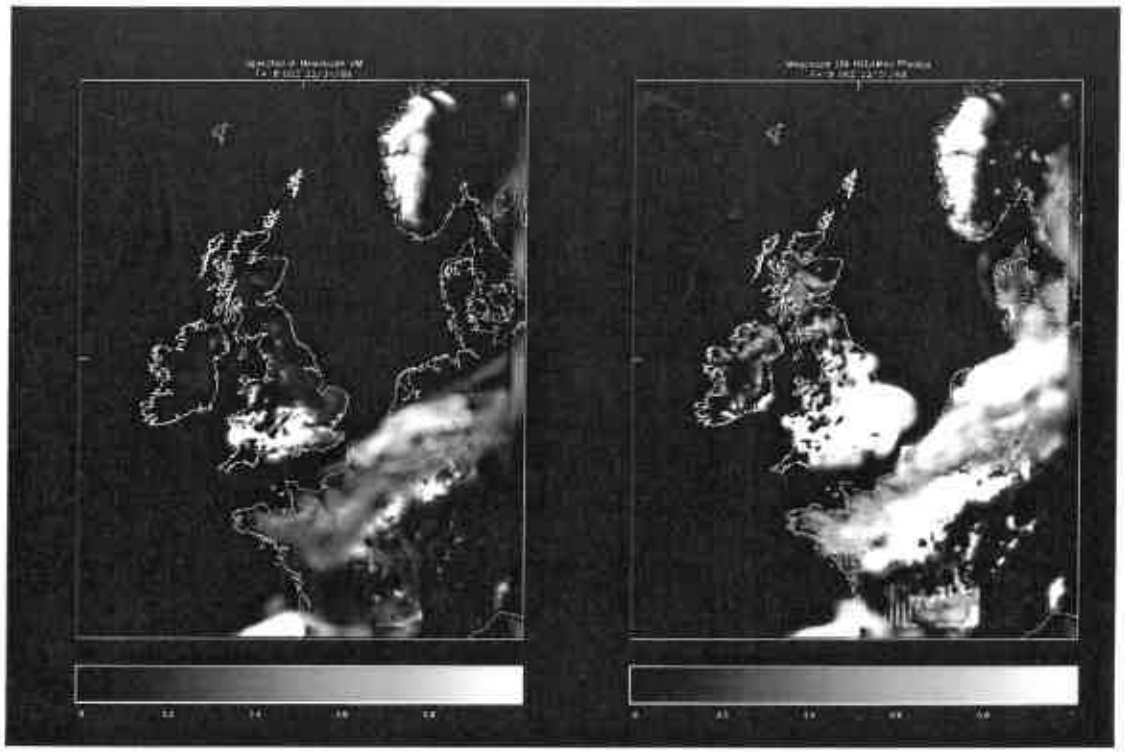

Figure 5 Screen level cloud fraction at 06Z 22/1/99, Operational UM on left, UM with HADAM4a physics on right

Past work has identified the advection scheme in the UM as a limiting factor for fog forecasting. This scheme requires an amount of diffusion to ensure numerical stability. Though switched off over 'steep' terrain, it still has an impact on UK stable fog. Since the diffusion is on model levels, which are terrain following, the effect is to diffuse up and over hills. In addition to the 'standard' UM configuration, additional runs were performed with modifications to the advection scheme. The first used a diffusion coefficient slightly less than ¼ that used operationally ($4x10^5$ compared with $1.9x10^6$, both 4^{th} order) . This is not advisable, and even in this run lead to unacceptable noise in the pressure field, but the model remained stable and produced a reasonable forecast otherwise. In more active conditions this would be unlikely to succeed. The third UM run used the positive definite tracer advection scheme for θ_L and q_t with a Superbee limiter. This has no explicit diffusion and generally retains gradients more effectively than the standard Huen scheme, at greater expense.

3.2 New Dynamics Configuration

The UM was run with Analysis Correction (AC) data assimilation from the 09Z analysis, and the 12Z analysis from the run with ND physics used to start the ND. This, of course, puts the ND at some disadvantage as the AC scheme continues to nudge in data beyond the nominal analysis time. An alternative would be to run with the model state 2 or 3 hours after nominal analysis time, as beyond 2 hours there is not further impact from observations. This was not attempted. For higher resolution runs the UM analysis was interpolated onto the new orography using the UM reconfiguration. The reconfigured analysis was then interpolated from the pressure-based UM vertical co-ordinate system onto the ND grid. This, too, is likely to have introduced some artefacts. Indeed, one of the major problems running the code was the production of negative cloud water or ice by the UM reconfiguration. Such small amounts were reset to zero with no attempt to conserve moisture. They appear to occur most frequently where new orography forces downward extrapolation into valleys.

The ND (version 2.7) was run at four horizontal resolutions. A global forecast was run to provide boundary conditions for the mesoscale model. The forecast was fairly indistinguishable from the UM global, which is not surprising to T+24, and, given the lack on importance of boundary data in this case, will not be discussed further. The mesoscale model was run with identical horizontal domain, grid and orography to the operational mesoscale model (roughly 12 km, 146x182 points). A 4 km domain (232x268) was embedded in the 12 km domain. This covered all Ireland and the UK apart from the Shetland Islands. Inside this was embedded a 2 km domain (266x240) covering the area shown in Fig. 2. The domains are shown in Fig. 6.

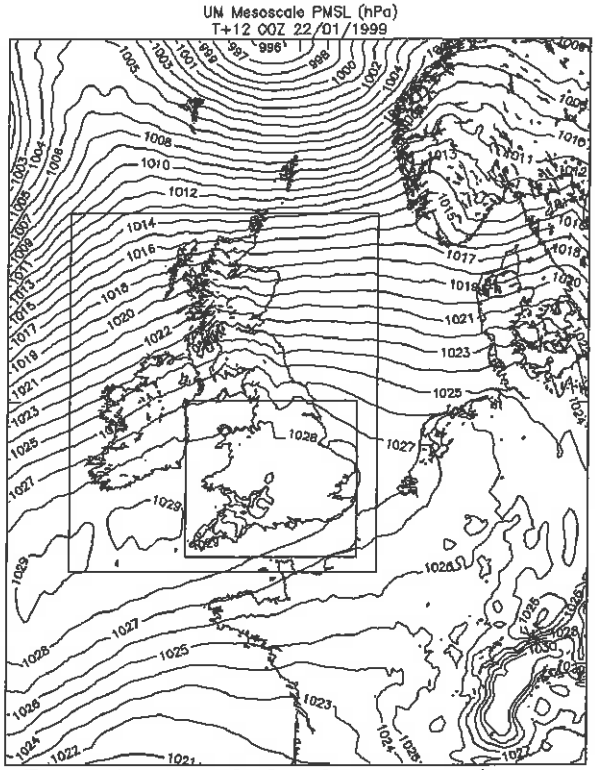

Figure 6 12, 4 and 2 km domains used in similations, together with the UM Mesoscale sea level pressure.

Orography was taken from an approximately 2 km resolution dataset derived from 100 m DTED data by Ian Culverwell. It is possible that some smoothing is therefore present at the highest resolution used. No additional filtering was employed. Land-use, soil and soil climatology data were taken from the standard UM ancillary system, and so have lower resolution than the model resolution used. Future work will investigate the impact of higher resolution land-use data.

The orography is illustrated in Fig. 7 for the area covered by the 2 km domain. Considerable additional detail is obviously added. At 12 km, only the major ranges of hills are identifiable, with Wales essentially one large barrier, and the Cotswolds, Chilterns, Mendips, North Downs etc. identifiable as (indistinct) features. The SW Peninsula is, essentially, one ridge with no major valleys except for the broad dip between Exmoor and Dartmoor. Notable additions from 12 to 4 km are river valleys through most of the major ranges. At 2 km tributaries to the main rivers are clearer.

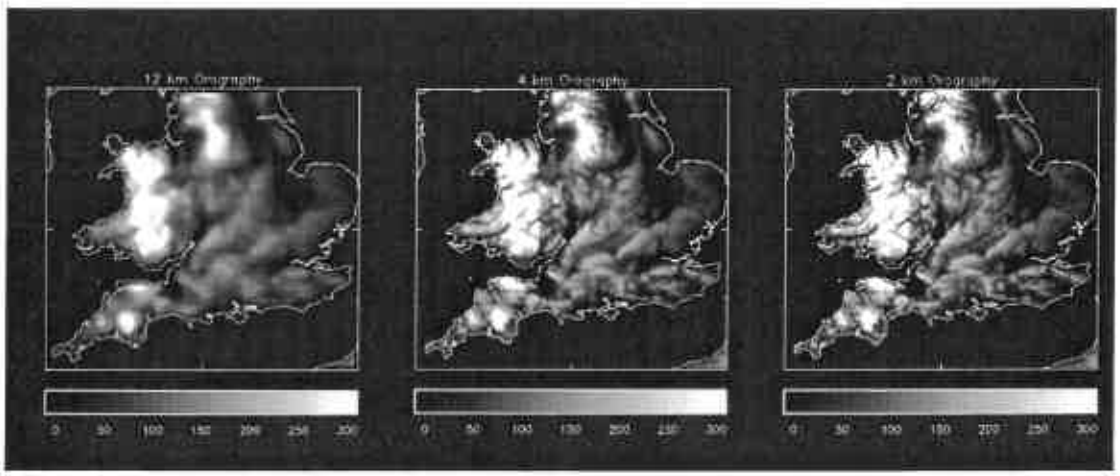

Figure 7 12, 4 and 2 km orography over 2 km domain.

The differences between different resolutions are shown in Fig. 8. A subjective impression of the 4 km – 12 km difference is that, as well as an underlying random signal, the major hills, particularly in England, show up quite distinctly. Many of these are quasi two-dimensional ridges or escarpments, so, as one might anticipate, the impact of going to higher resolution is to sharpen, and increase the height of, such ridges. This is of particular significance when considering the Froude number of the flow with respect to the ridge height, and assessing the likelihood of blocking. The difference between 4 and 2 km orography is, as expected, less marked.

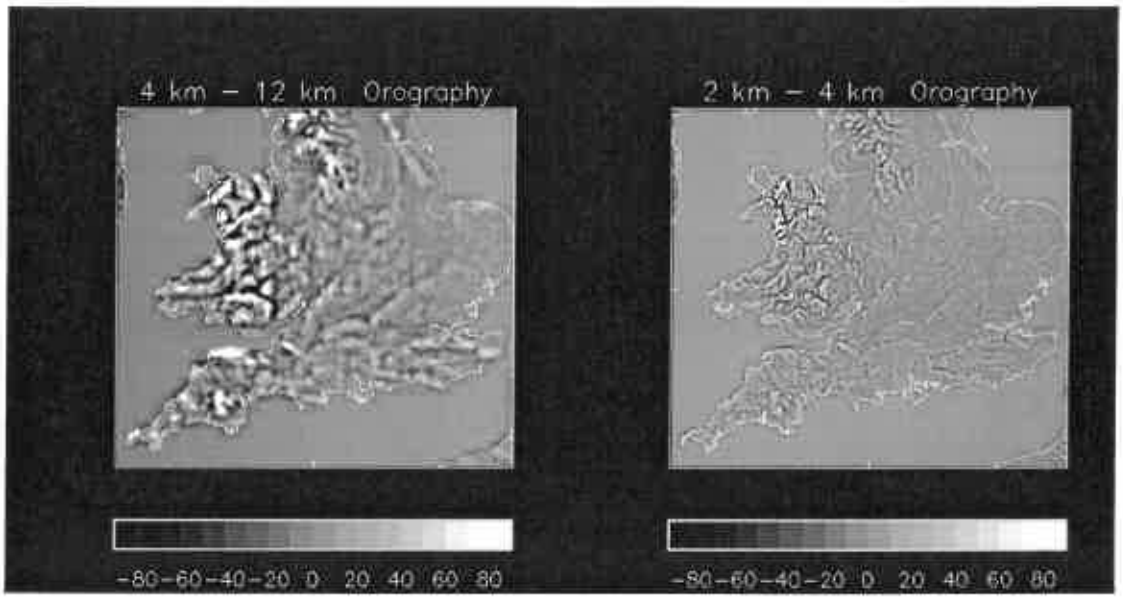

Figure 8 Differences between 4 and 12 km (left) and 2 and 4 km (right) orography.

Initially all were run with 38 levels corresponding closely in height to the mean heights of the operational UM mesoscale model, though, of course, it is impossible to maintain exact correspondence. It is likely that better vertical level distributions, with smoother distribution and, on the whole, poorer boundary layer resolution, are possible for the ND from the point of view of accurate dynamics, but, in this case, boundary layer behaviour is thought to be at least as important.

The Charney-Philips grid is, for radiation fog, perhaps a greater concern, particularly regarding radiation. In the UM, with a bottom level at approximately 10 m, the radiation scheme sees a temperature appropriate to 10 m and estimates the radiative heating and cooling for a 20 m thick layer. On the Charney-Philips grid, if the bottom wind level is at 10 m, the lowest temperature level (above the surface) is about 20 m, and the radiation scheme sees a layer about 40 m thick. The variable grid thus reduces the effective resolution near the surface for the radiation scheme. An alternative view is that, while radiation increments are calculated on theta levels, no account is taken of the surface being a theta level, so the first theta level above the surface is effectively treated as being one and a half layers thick. A vertical grid with 45 levels was also used to assess the importance of this. The lowest levels of the two grids are shown in Table 1. This shows the there is a rough correspondence between the θ level heights of the 45 level model and the density level heights of the 38 level model.

Level	38 Levels		45 Levels	
	Density level height	θ level height	Density level height	θ level height
1	10.5	21.1	4.4	8.7
2	42.2	63.4	21.8	34.9
3	105.9	148.6	56.7	78.5
4	202.2	256.0	109.0	139.6
5	321.1	386.4	178.8	218.1

Table 1 – Lowest level heights in New Dynamics Runs

3.3 *Model technical details, problems and solutions*

All ND runs used ND version 2.7, with a number of modifications at the control level, mainly associated with production of boundary data, which brought the code close to 2.9. All were run on T3EA; the limiting factor with the high resolution runs tends to be processor memory rather than (in a non-operational context) CPU. All used α values of (0.7,1.0,0.7,1.0).

Resolution	12 km		4 km		2 km	
Levels	L38	L45	L38	L45	L38	L45
Timestep	300s	300s	120s	120s	60s	60s
Radiation timestep	3600s	3600s	1200s	1200s	600s	600s
Boundary updating	3 hour	3 hour	1 hour	1 hour	1 hour	1 hour
Diffusion coefficient	1.4E3 (top 2 levels only)	1.4E3 (top 2 levels only)	6.8 E3	6.8 E3	3.158E3	3.158E3
Diffusion order	1 (top 2 levels only)	1 (top 2 levels only)	2	2	2	2
Processors	48	48	96	96	96	96
Total CPU (seconds)	171800	230200	900400	1021100	1187500	1577900
CPU Per Processor (approx)	3600	4800	9400	10600	12400	16400
Max memory (Mwords)	370	415	900	1003	920	1040
GCR abs tolerance	5.0E-3	5.0E-3	5.0 E-4	5.0 E-4	1.0E-4	1.0E-4
Typical solver iterations	20	24	24	28	40-50	70

Table 2 Significant configuration and run parameters in New Dynamics runs.

The 12 km runs used the same Rhcrit values in the cloud scheme as the UM. After some experimentation, a value of 0.96 was used in the bottom 8 (of 38) and 12 (of 45) levels , with 0.85 above in the higher resolution runs. While this has some impact on the verification, the overall evolution is largely unaffected by the choice of this parameter. A lower value near the surface leads to more diffuse edges to the fog, but little more. Similarly, the radiation scheme was called more frequently. This was regarded as prudent, but, in fact, had little impact compared with calling hourly, as the cloud distribution does not change very much in this time.

Choice of diffusion coefficient is more significant. When initially run, no diffusion was used (except at the very top of the model) and the 4 km runs showed unphysical behaviour at one point in the Lake District. This point is relatively low (near Keswick) but surrounded by high ground. Surface and near surface temperatures showed excessive cooling, the surface eventually reaching about 160K at the end of the night. Not surprisingly, this eventually influenced other gridboxes, but as winds were light, the problem did not spread until the cold air had deepened enough to 'spill' out of the valley, after which cold 'plumes' were transported away. It is, perhaps, a tribute to the dynamics that no numerical problems arose.

Experiments were performed with rapid radiation timesteps, to no avail. It is believed that the problem arose from a known simplification in the MOSES surface exchange scheme. At present, as surface temperatures adjust in the scheme, the net longwave radiation is not corrected in a timestep. Thus, the outgoing radiation calculated with a high initial temperature is not reduced as the surface rapidly cools. An improved scheme has been implemented by MP branch but it is not available in the ND (yet).

The same phenomenon has been observed in the single column model, but not in the UM. A possible reason for this is that diffusion sufficiently couples the air to adjacent grid boxes that the instability in the surface exchange is controlled. Addition of diffusion to the ND was found to remove this extreme behaviour. The values chosen represent e-folding times of about 750 and 390 s in the 4 km and 2 km models, or just over 6 timesteps in each case. Apart from the area in question, no visible impacts were evident in the fog distributions. This suggests that running with this amount of diffusion may be a good compromise for controlling gridscale noise while not introducing excessive dissipation. (For information, a value of 2.4E4 would have an e-folding time of about 6 timesteps in the 12 km case).

3.4 Verification methods

The ND code contains neither the aerosol prognostic or the visibility diagnostic of the UM. In fact, few screen level diagnostics are available routinely. The screen level cloud fraction, RH, liquid water and ice are produced but not output, so the code was modified to produce these. In the absence of the prognostic aerosol, a strictly comparable visibility could not be produced, so no effort was made to add the visibility diagnosis to the code. Previous work (Clark, 1993) has shown that the 'probability of visibility less than 1000 m' is a better indicator of fog than the median visibility. The cloud fraction at screen level is close to this, though slightly less in magnitude. The cloud fraction at screen level was therefore used as a surrogate indicator for fog. This may (perhaps) be compared with visibility observations. A threshold value of 0.3 was used as a 'fog/no fog' discriminator, though the value of this threshold was not too critical. This was interpolated to measurement sites and compared with observed visibility less than 1 km.

Cloud fraction at screen level may not be such a good variable to compare with satellite imagery, as fog that is a little lifted to stratus in the model or reality will also show up in the imagery. As a surrogate for the satellite imagery, a total liquid water path was derived by integrating through the boundary layer. In the event, there was no cloud above the boundary layer in the model in the regions of interest. Within the dynamics, the correct algorithm to use to ensure consistency and conservation is a subtle issue which will not be considered here. However, for the, largely qualitative, diagnostic purposes here a simple algorithm was adopted. In the UM, the mixing ratio is assumed representative fixed in a layer, so the total liquid water is derived from the total mass of air in a layer assuming the pressure thickness is related to the mass by the hydrostatic relationship. This is consistent with the UM and leads to:

$$lwp = \sum_{k=1}^{n} q_{cl} |\Delta p_k| / g \qquad (1.1)$$

Similarly, in the new dynamics, the mass in a layer is taken as the mean density times layer thickness in m, and the mass of liquid water derived by multiplying this mass by the mixing ratio. This is an approximation, but at the percentage level. It is thus regarded as adequate for qualitative comparison with the UM and more so for comparison between ND runs as any errors are likely to be systematic. This leads to:

$$lwp = \sum_{k=1}^{n} q_{cl} \overline{\rho} \Delta z_k \qquad (1.2)$$

The layer depth is taken to be the distance between adjacent density levels. However, the layer depth for the first layer is ambiguous as moisture variables are stored at the same points as θ. In order to improve (slightly) the diagnosis, the value derived at 'screen' level has been used for the first 'half layer', i.e. surface to first density level. This should not be regarded as the appropriate scheme to use when considering conservation, but is regarded as a good estimate for diagnostic purposes.

3.5 Fog Results

The evolution of fog in each run was complex and time varying. Indeed, it is a feature of all the runs that there was considerably more variation from hour to hour than suggested by the observations. The results have been summarised pictorially using data at 18Z 21/01/1999 and 00Z, 06Z and 12Z 22/01/1999, for screen level cloud fraction and liquid water path (Figs 9-12). The former shows the presence of fog, the latter (for comparison with imagery) indicates whether fog is absent because it has lifted into stratus or dissipated.

Equitable threat scores have been derived, as a function of forecast time, for each run, using the criteria for fog outlined above (30% forecast screen level cloud fraction, 1000 km observed visibility). These are shown in table 3.

Forecast Time	UM 12km	UM Lo Diff	UM Tracer	12km L38	12km L45	4km L38	4km L45	2km L38	2km L45
3	0.099	0.084	0.233	0.049	0.049	0.049	0.049	0.099	0.202
6	0.159	0.177	0.183	0.193	0.193	0.191	0.346	0.080	0.291
9	0.094	0.054	0.089	0.270	0.205	0.303	0.257	0.321	0.223
12	0.082	0.076	0.076	0.210	0.167	0.206	0.171	0.179	0.075
15	0.065	0.085	0.035	0.135	0.113	0.197	0.136	0.196	0.120
18	0.095	0.102	0.040	0.141	0.110	0.151	0.088	0.110	-0.022
21	0.129	0.135	0.121	0.201	0.116	0.043	0.083	0.067	0.023
24	0.175	0.167	0.175	0.047	0.038	-0.003	-0.028	0.017	0.000

Table 3 Equitable threat score of observed fog (defined as visibility less than 1 km) against forecast (defined as screen level cloud fraction greater than 30%).

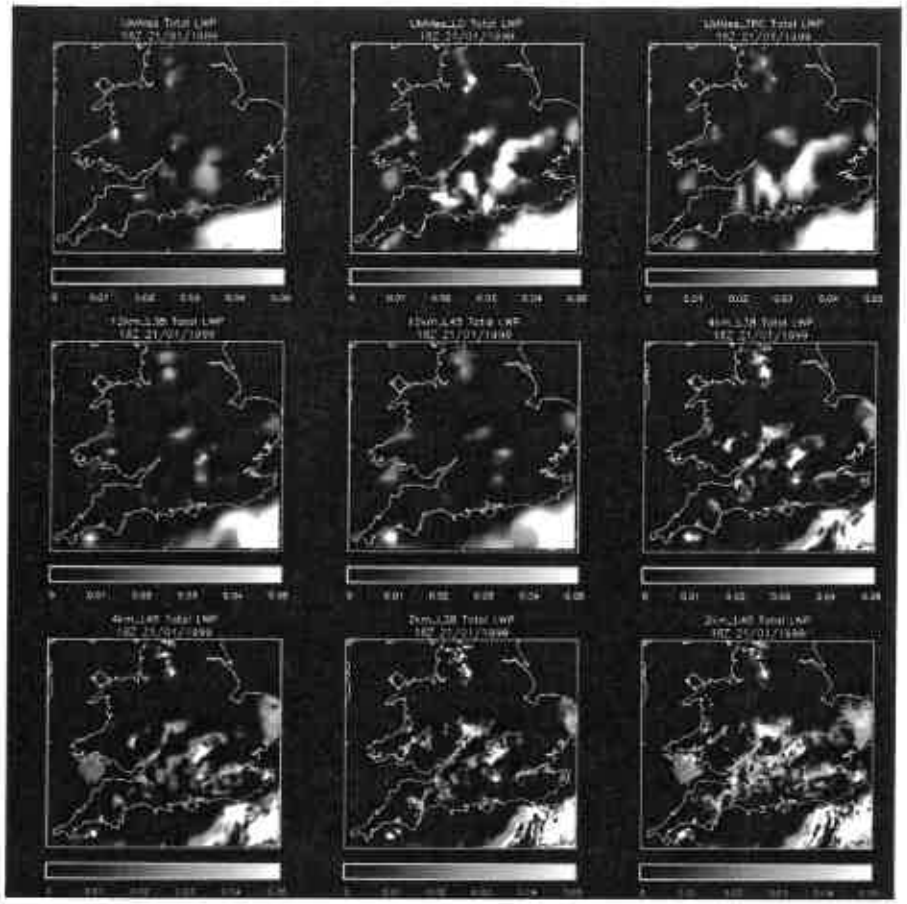

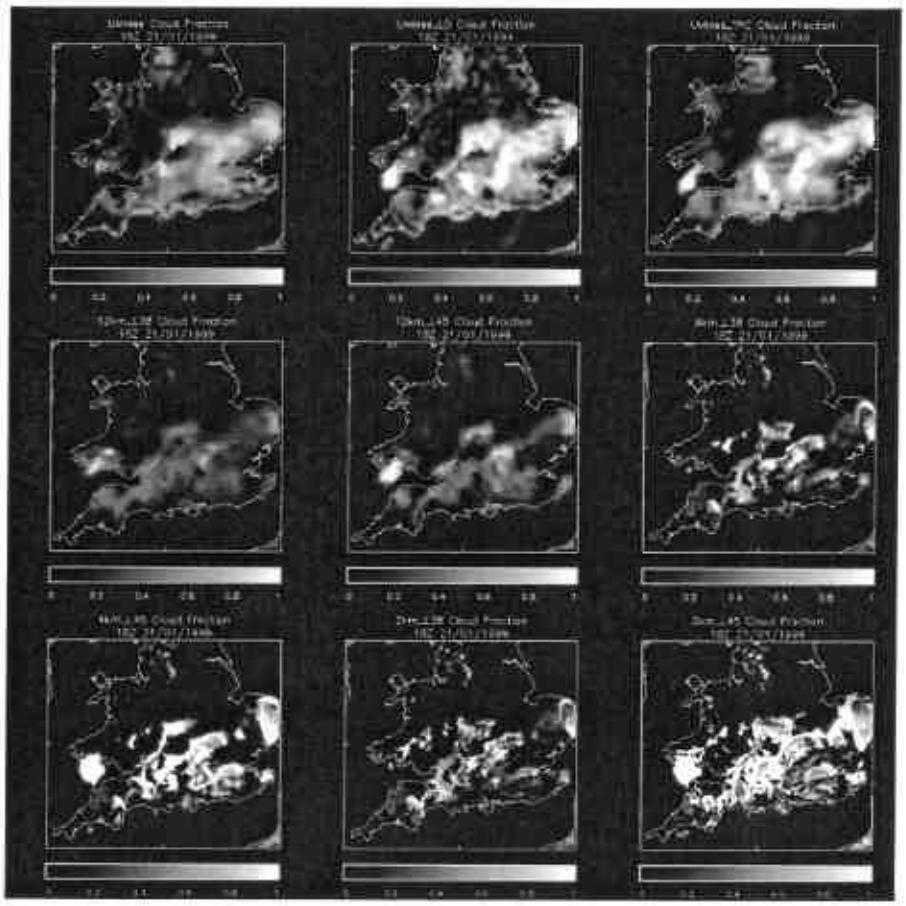

Figure 9 Screen level cloud fraction (top) and total LWP (bottom) at 18z, 21/1/99

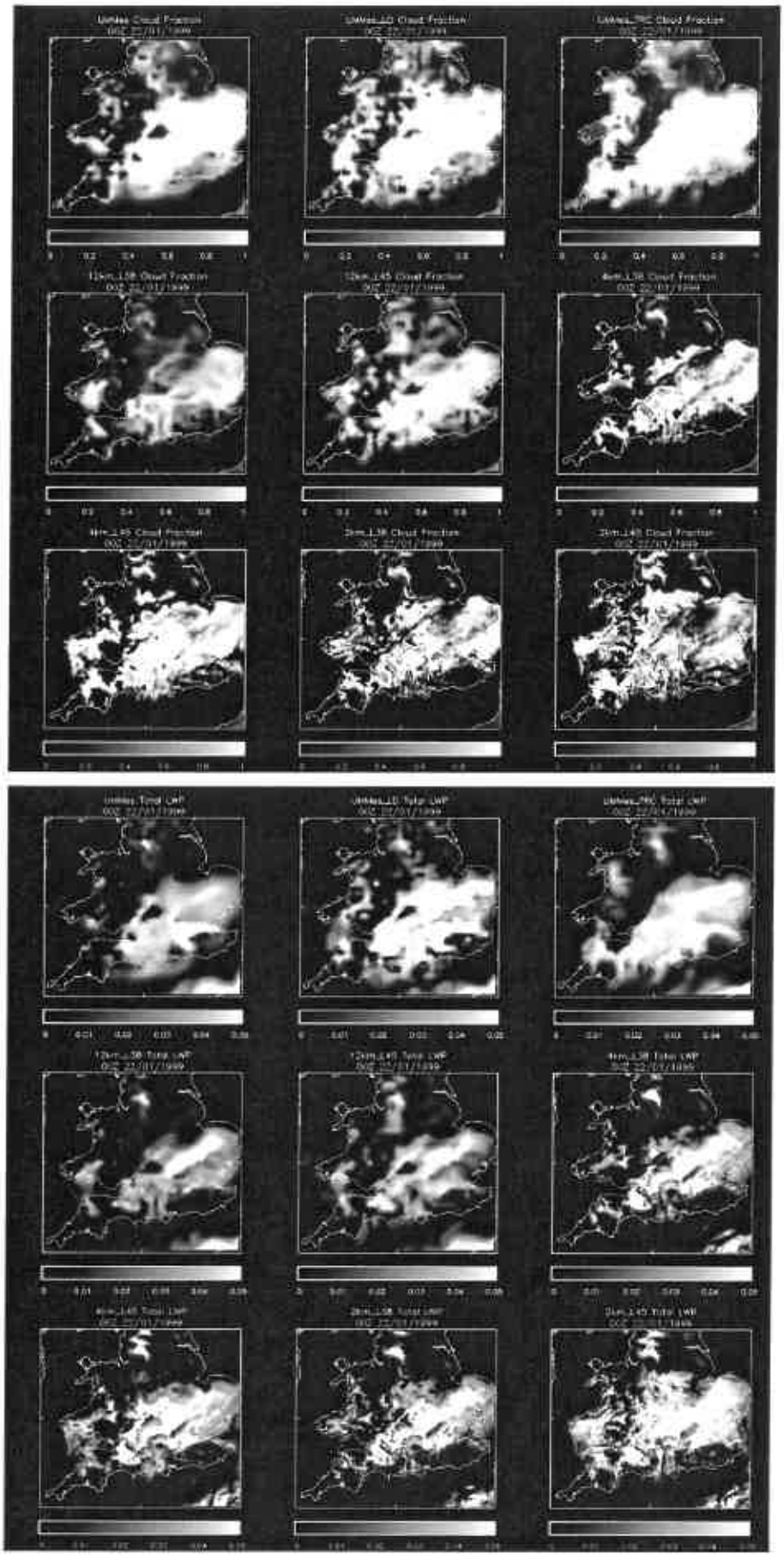

Figure 10 Screen level cloud fraction (top) and total LWP (bottom) at 00z, 22/1/99

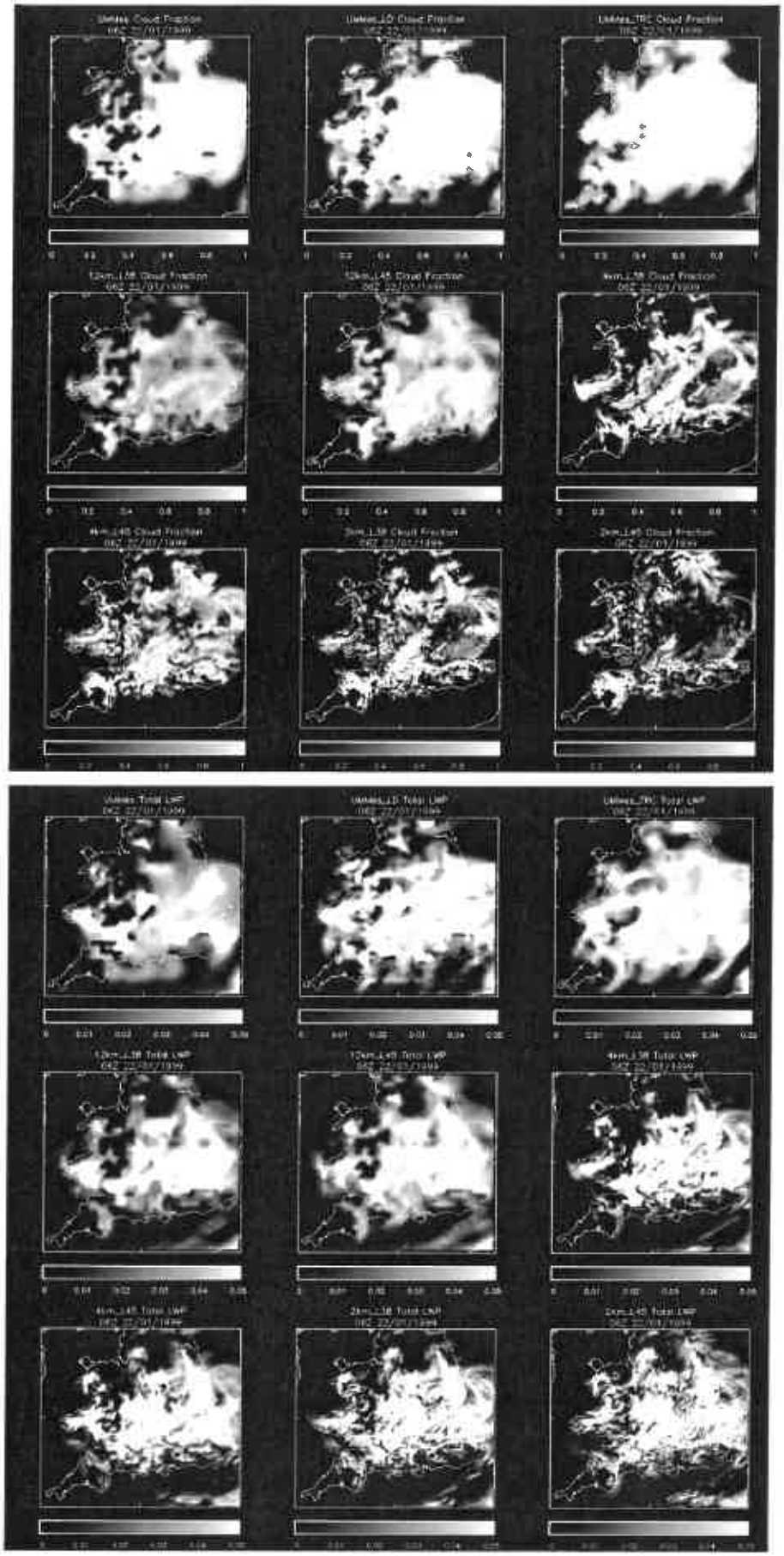

Figure 11 Screen level cloud fraction (top) and total LWP (bottom) at 06z, 22/1/99

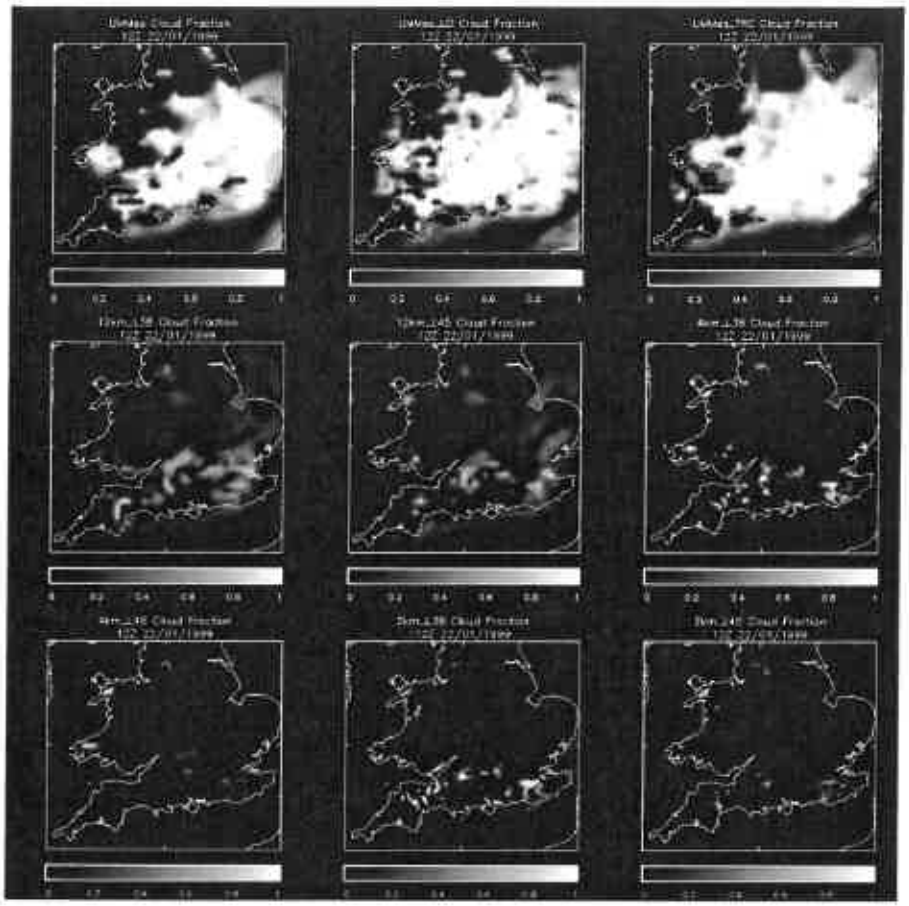

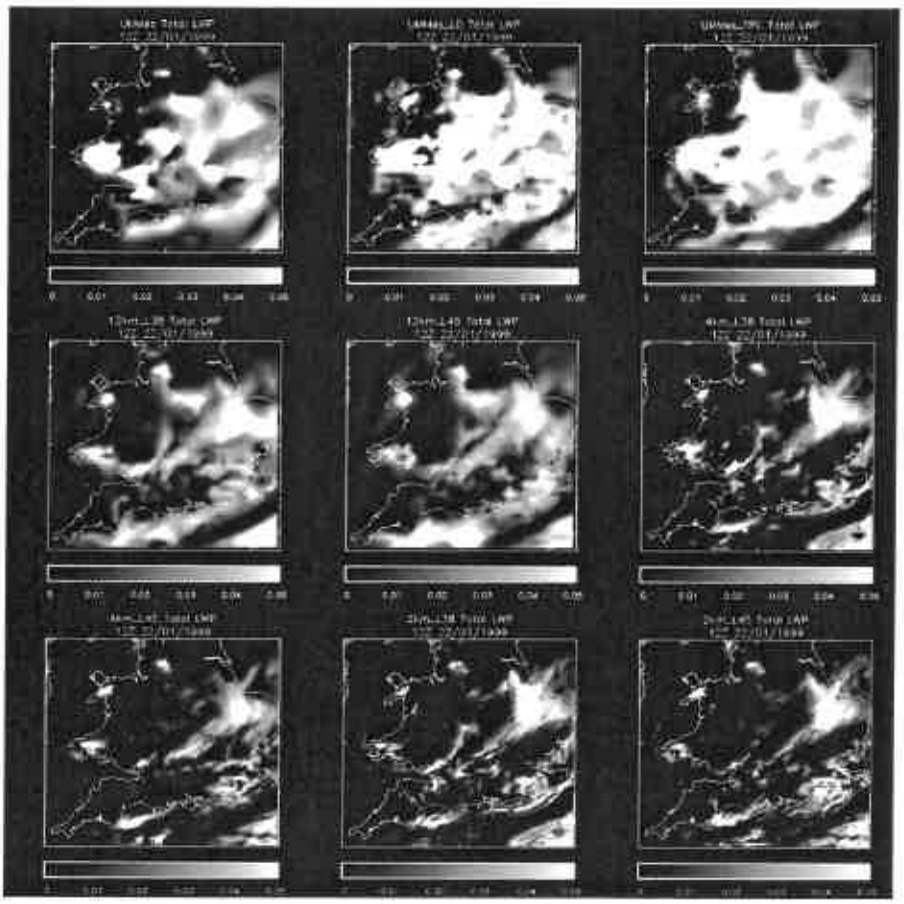

Figure 12 Screen level cloud fraction (top) and total LWP (bottom) at 12z, 22/1/99

3.6 Model Winds

Verification against observations is probably of little value in extremely light winds. Some information may perhaps be gained if any trends become obvious. At high resolution, displaying the wind field that develops around the complex topography becomes very difficult. Figs. 13 – 15 show the wind field at 10 m above orography for a small section of central England featuring the Severn/Avon valley, the Cotswolds and Chilterns. The diagonal line marks the position of the cross sections discussed below. Even over this small area, the data have been thinned such that every second point is shown in the 4 km runs and every third point in the 2 km runs. All the ND runs show more coherent, organised flows, generally stronger, at least at later times. In the ND case, winds have been interpolated linearly to 10 m from the model level data. In the UM case, level 1 is used as this has a mean height of 10m above orography. The 10 m wind derived in the UM from the boundary layer profile is not used.

In the early evening there is a SW flow over most of the area, especially up the Severn and Avon valleys, but with a clear flow diffluence along the ridge of the Cotswolds, with down slope flow. In the ND, there is SW flow around Oxfordshire, between the Cotswolds and Chilterns and all runs show flow off the Chilterns into the Thames valley. By 00Z, the flow has become a little more westerly. The UM shows evidence of down slope flow off the Cotswolds, though, interestingly, this is less pronounced in the low diffusion and tracer advection runs. The higher resolution runs show plausible response to relatively small valleys, which would have important local implications but are hard to verify. They also show generally stronger winds. By 06Z the discrepancy between the ND and UM runs is clear, with much stronger SW flow in the ND. This probably accounts for the poor fog performance at this and later times, as there is sufficient wind to lift and advect the fog.

Examination of the mean sea level pressure (MSLP) shows little significant difference between the runs on the synoptic scale (though there is, perhaps, a tendency to be up to a hPa higher overall in the ND), but small scale gradients are significantly higher, which probably accounts for the stronger winds. Thus, it seems reasonable to suppose that the ND is generating slightly stronger thermal gradients associated with the orography and hence a stronger overall response which *may* be excessive. However, the possibility of a more serious, large scale problem, should not be discarded. The possibility also exists that the difference is as a result of different synoptic scale development resulting from the earlier effective cutoff in the data assimilation period, or from reconfiguration artefacts.

These problems are reflected in table 4 which shows RMS vector wind errors for sites within the 2 km model domain. Vector wind error is more useful with light winds, as a pure direction error can be misleading. All are reasonably good, but the ND runs show a distinctly worse performance compared with the UM, consistent with the view that winds are a little too strong. In this case, there is clear benefit from higher vertical resolution and little from horizontal, though this probably reflects both the sparseness of the data and the choice of sites.

FT	UM 12 km	UM Lo Diff	UM Tracer	12km L38	12km L45	4km L38	4km L45	2km L38	2km L45
3	1.62	1.60	1.59	1.83	1.62	1.91	1.67	1.91	1.68
6	1.43	1.42	1.42	1.97	1.54	1.95	1.51	1.90	1.53
9	1.38	1.37	1.37	1.60	1.40	1.68	1.42	1.65	1.47
12	1.48	1.52	1.52	1.74	1.60	1.86	1.71	1.90	1.78
15	1.44	1.53	1.47	1.75	1.61	1.79	1.69	1.81	1.64
18	1.44	1.51	1.44	1.86	1.68	1.93	1.77	1.91	1.79
21	1.42	1.49	1.42	2.17	1.89	2.06	1.75	2.08	1.79
24	1.42	1.50	1.44	2.14	1.95	2.23	1.98	2.27	1.99

Table 4 RMS Vector wind errors over the domain covered by the 2 km model

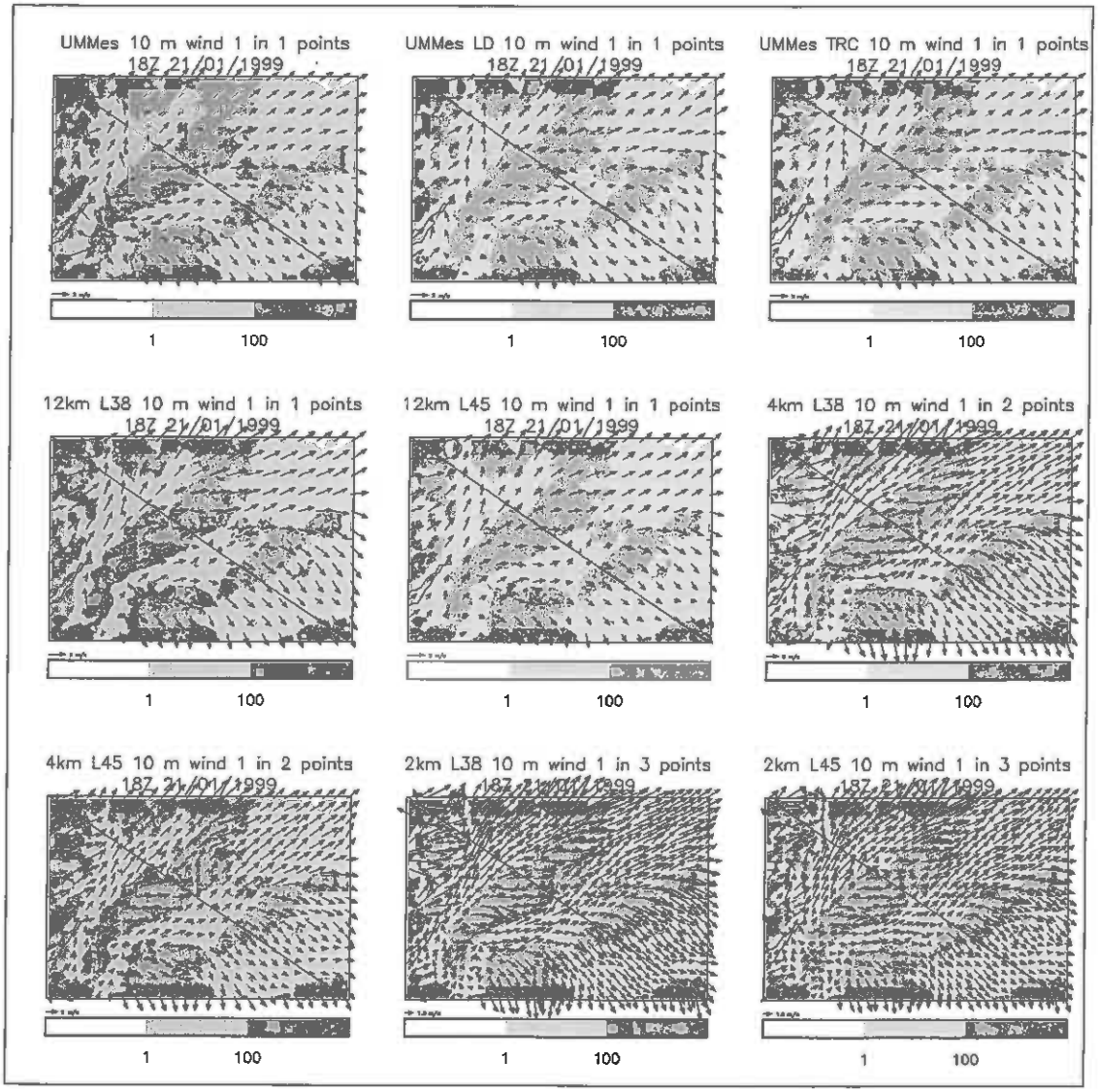

Figure 13 10 m wind over central England, 18Z 21/1/99. Equal scales on all plots.

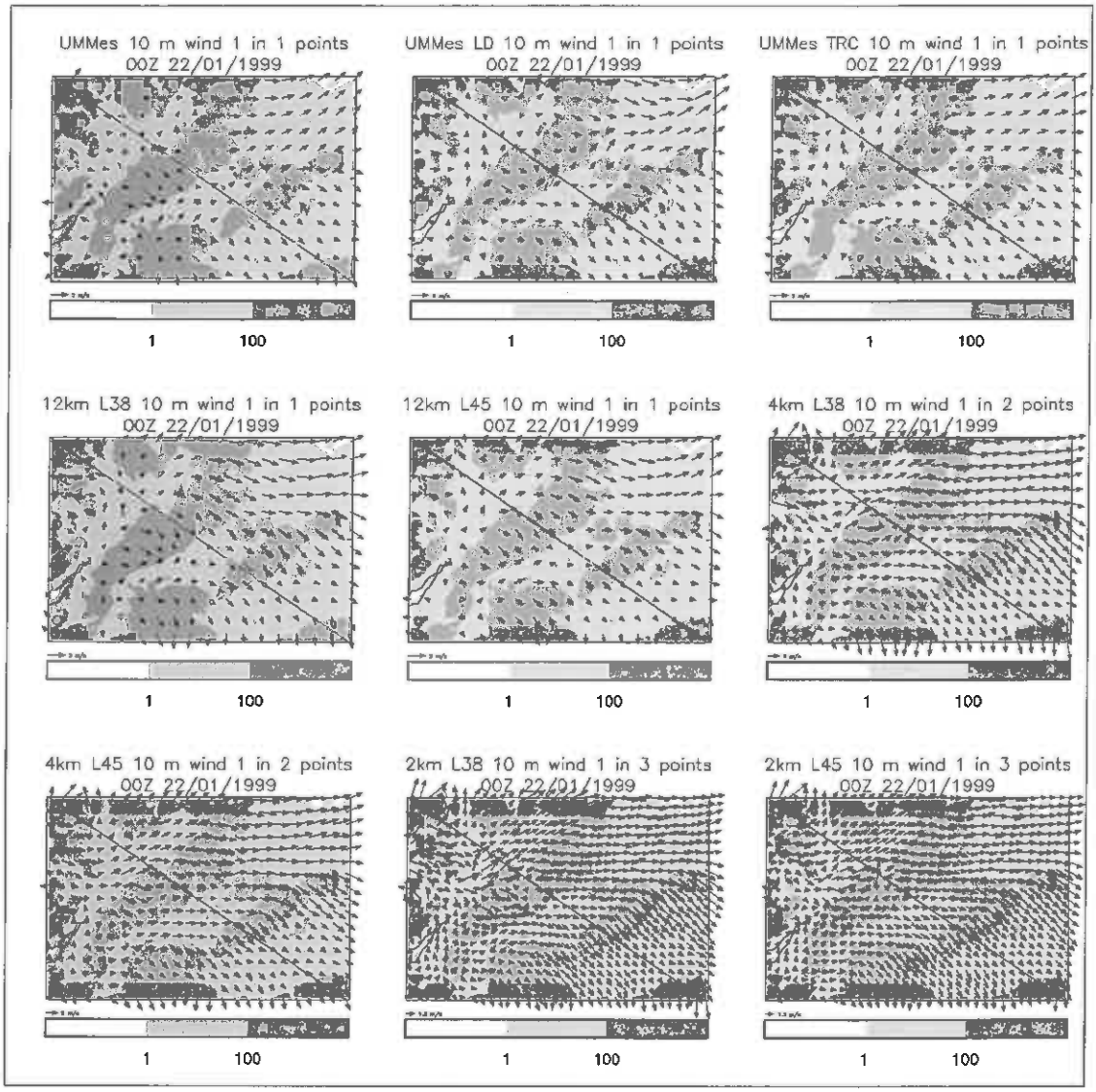

Figure 14 10 m wind over central England, 00Z 22/1/99

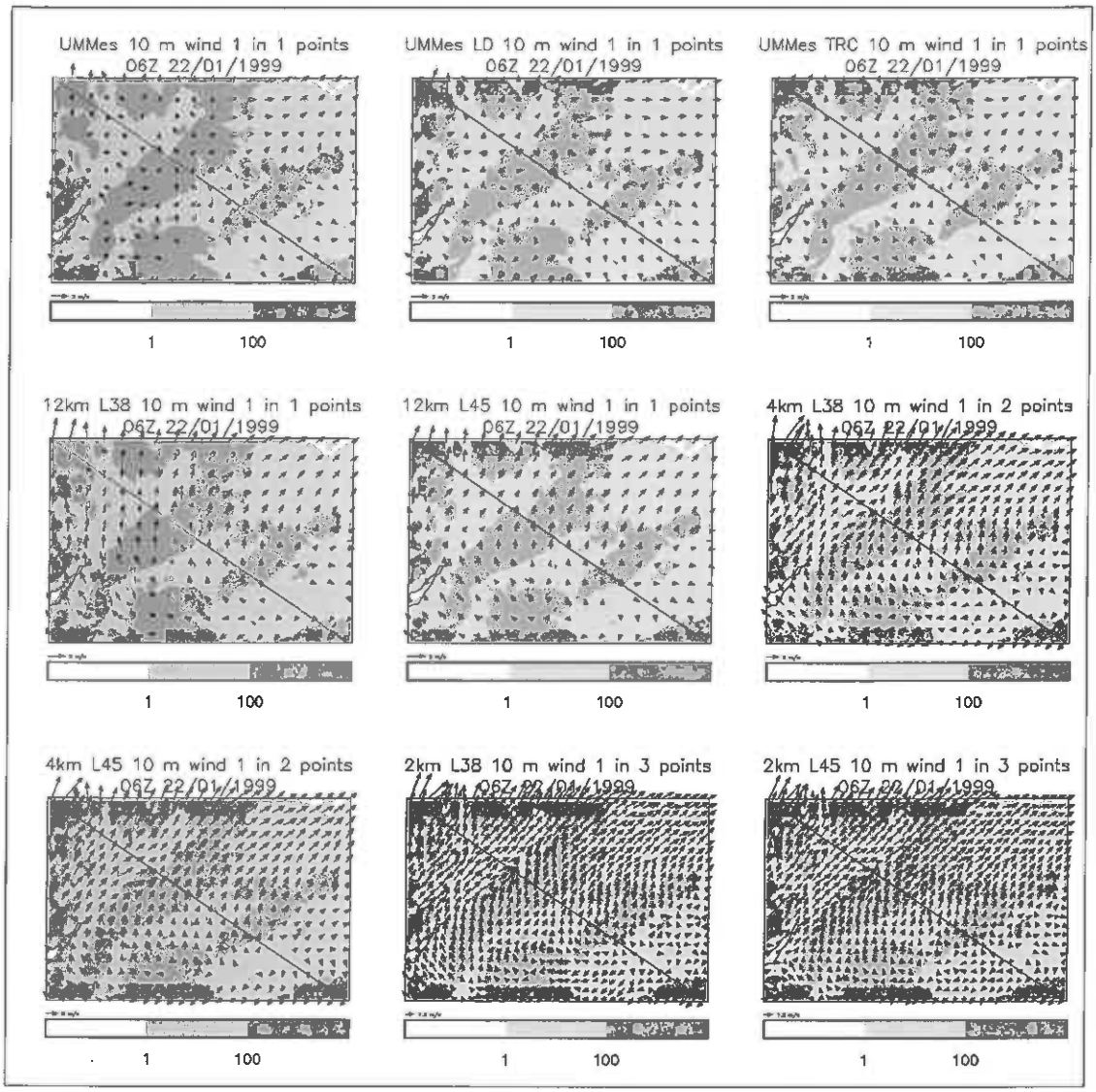

Figure 15 10 m wind over central England, 06Z 22/1/99

It is also of some interest to look at the SW Peninsula. This is shown at 00Z in Fig. 16. Notable features are convergence lines presumably associated with the outflow of cold air from land over the sea (i.e. land breezes). The UM does not exhibit much of a feature (though one develops later and also in the Channel). With reduced diffusion or tracer advection the feature to the NW is much more marked. Again, verification is fairly pointless, but it is encouraging that directions and strengths of coastal winds are quite good, and the locations of near calms in reasonable agreement with the few observations. It is interesting to note that the position of the convergence line out to sea seems to depend much more on vertical than horizontal resolution, with more penetration in the higher resolution runs consistent with more effective cooling over land. The imagery in Fig. 1 shows evidence of a convergence line to the W of Great Britain which may be associated with this feature, in which case the 45 level positions verify better. There are also features emanating from the Exeter region which are associated with traces of fog in the model and in imagery.

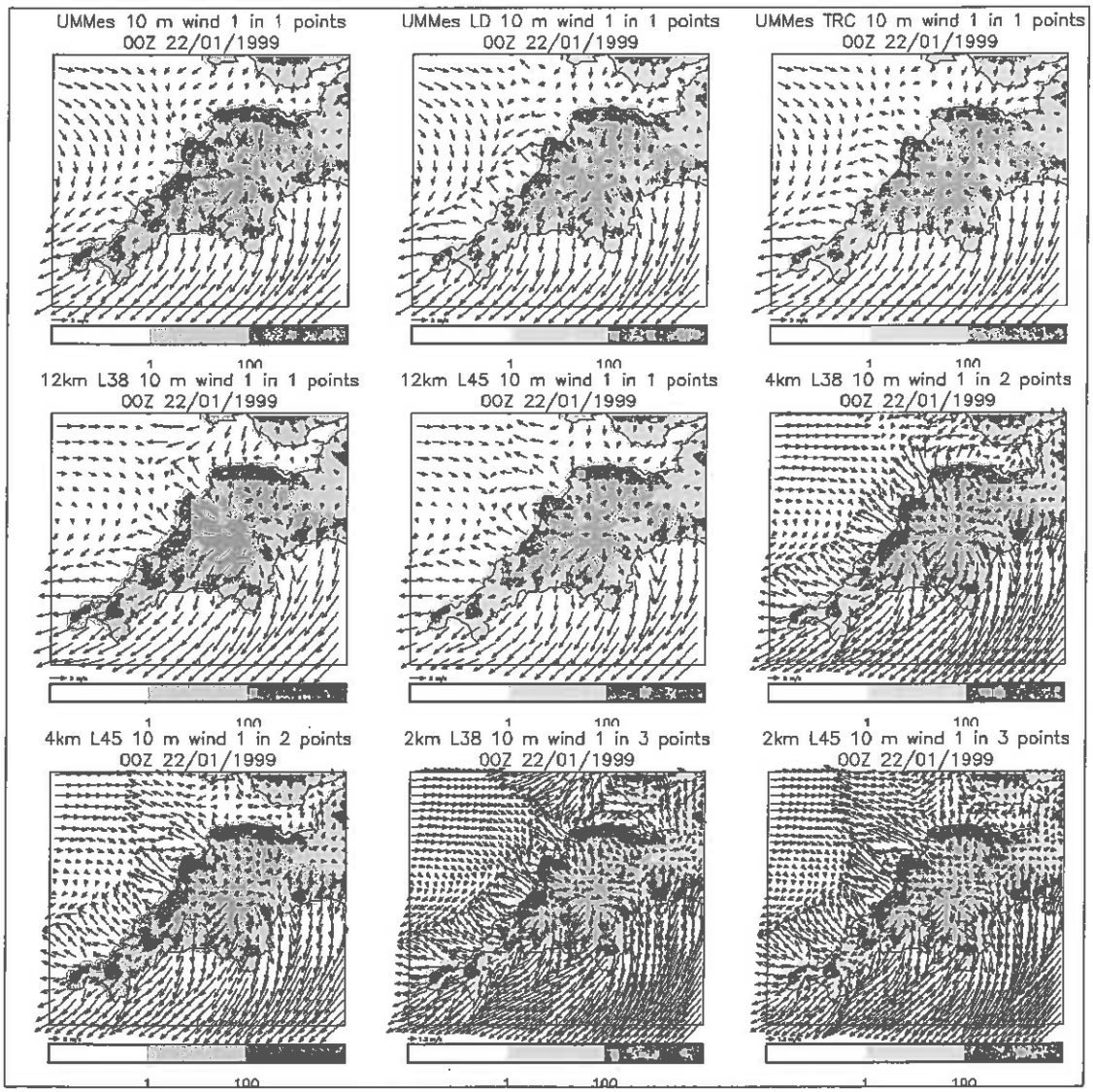

Figure 16 10 m wind over SW England, 00Z 22/1/99

3.7 Cross sections

It is instructive to look at cross sections through central England. The section shown in Figs 13-15 has been chosen as it intersects the main fog areas and in roughly perpendicular to the orography. Cross sections of potential temperature and cloud fraction are shown in Figs 17 and 18 at 18Z 21/1/99 and 00Z, 06Z and 12 on 22/1/99. These cross the Severn and Avon valleys, the Cotswolds, then Chilterns into the Thames valley and finish at the North Downs. The interest here is in the ND performance with resolution, so for reasons of space only the ND runs are shown. These have been plotted using model level data, and the bottom boundary is actually the bottom model level, rather than the surface.

The first thing to note is the general depth of the fog forecast. Although we have no direct measure of the fog top, the imagery seems to strongly suggest a relatively flat top at about 100-120 m amsl. In the 38 level runs, the early fog formation extends up to 300m by 18Z. The main boundary layer temperature gradient starts above 200 m, with fairly uniform temperatures beneath. At higher horizontal resolution, the fog is thicker and, as one might expect, has better defined edges. There seems to be a tendency to produce more valley fog as the resolution increases. It is noticeable that fog forms on the northern edge of the North downs rather than in the Thames valley, probably as a result of the (relatively) strong SW flow off the Chilterns, though, perhaps, also because of enhanced surface roughness. At higher vertical resolution, the initial fog formation is distinctly shallower. This was the anticipated impact, but does not show up so clearly in the surface fog or the total water path; Presumably the latter represents an overall cooling which is independent of resolution.

By 00Z, the distinction is not so clear, with fog having grown deeper in the higher resolution runs. Indeed, the 45 level runs show increasing depth with higher horizontal resolution and rather more resolution sensitivity than the 38 level runs. In all cases the fog depth in the valleys is higher than the surrounding hills, and some fig is present on hill tops.

By 06Z these trends have increased, to the extent that in all the higher resolution runs the fig has lifted to a stratus deck, the most extreme being the 2 km, 45 level run with top above 400m, compared with the 300m top of the 12 km runs (which still have fog on the surface). By 12Z the lifting has completed and distinct stratocumulus decks are found above each valley.

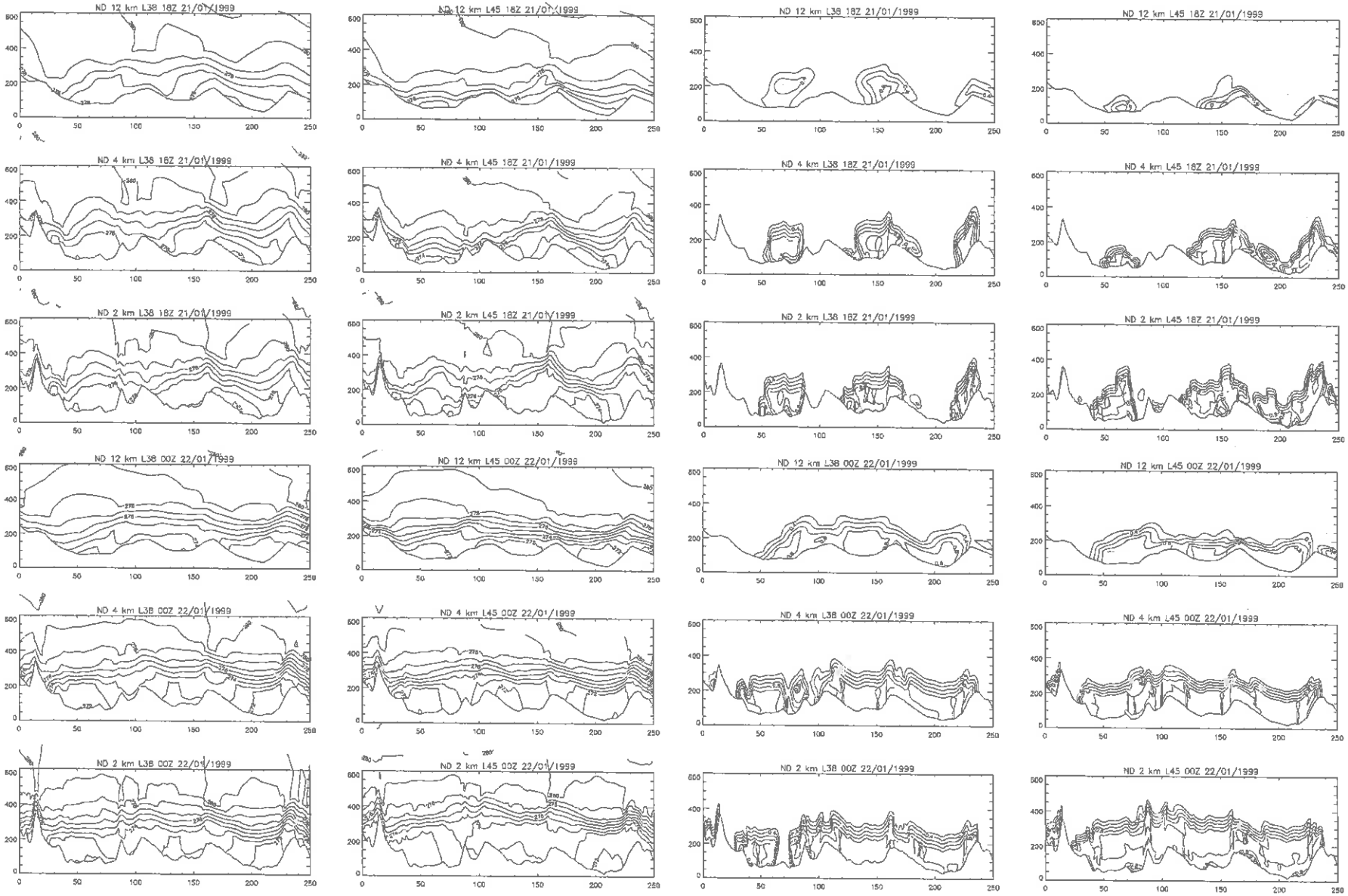

Figure 17 Cross sections through theta (left) and cloud fraction (right) for 18Z, 21 (top) and 00Z 22/1/99 (bottom)

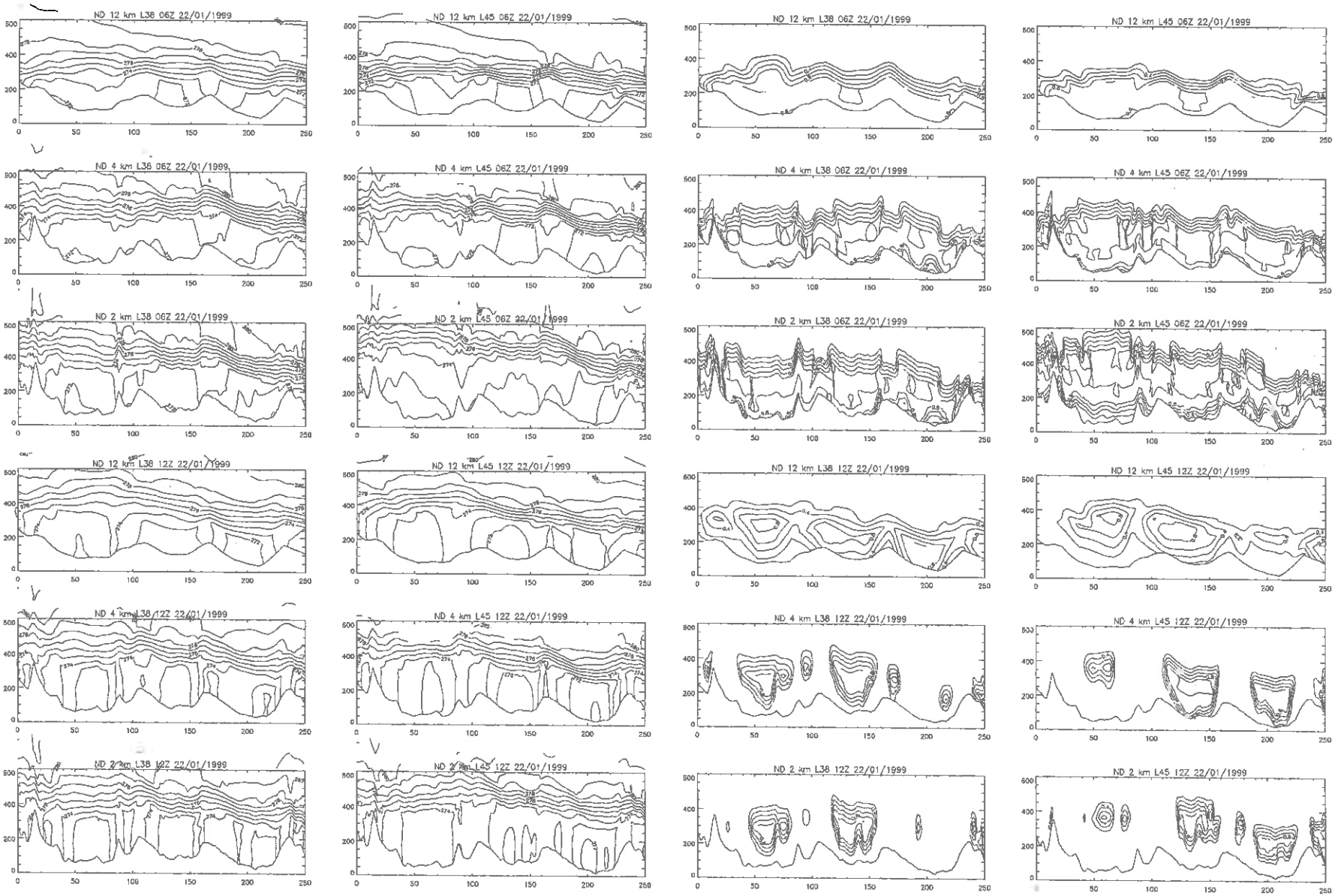

Figure 18 Cross sections through theta (left) and cloud fraction (right) for 06Z (top) and 12Z 22/1/99 (bottom)

3.8 Discussion

A number of points from the subjective comparison and the objective scores are noteworthy:

- The UM generally predicts more widespread fog and low cloud than the ND. In general, this may not be desirable at all times, but there seems little doubt that for the last few hours of the forecast, the ND is predicting too little fog or low cloud.

- The 12 km ND fog verifies better objectively than any of the UM runs except at T+24.

- The difference in objective score between ND and UM at 12 km is substantial and much larger than the impact of changes to the advection scheme in the UM.

- Differences between the 38 and 45 level ND are significantly smaller than between UM and ND.

- The 45 level ND at 12 km is objectively worse than and subjectively similar to the 38 level ND. More fog and low cloud is produced in the 45 level case, which probably accounts for the lower score.

- The higher resolution runs do not, universally, verify objectively better than the 12 km ND. They are broadly similar, with some pluses and some minuses.

- The early stages of fog formation (up to T+9 and perhaps T+12) are well captured by all the ND runs, and especially the higher resolution models. In these stages the screen level fog is more sensitive to vertical resolution, and the 45 level model performs better than the 38 level model. The early (to T+6) objective performance of the 2 km, 38 level model compared with the 45 level model shows the potential for objective verification problems. The 38 level run is developing more slowly, but the difference between the two fields subjectively probably does not warrant the substantial difference in score, especially when one looks at the 4 km 38 level run which resembles the 2 km 38 level run but verifies much better. Clearly, at such a critical stage, the additional detail at higher resolution can be misleading.

- All runs show evidence of blocking by orography. During the formation stage, up to 00Z (T+12), the higher resolution runs are particularly impressive when compared with imagery. This is encouraging for data assimilation, as the background field should be more representative of the individual observation sites. However, while the region affected by fog is clearly delineated, even at T+3 the forecasts probably have too deep a fog layer, extending above 200m (lower in the 45 level runs than the 38).

- In the later stages, the higher resolution models lift, and, ultimately, dissipate the fog more rapidly than the 12 km ND runs, which, themselves, do so more rapidly than the UM. The lifting appears to start in the Bedfordshire/Cambridgeshire region and propagate outwards. There is also a subjective impression of an excessive eastward drift in the Midlands. Both higher horizontal and vertical resolution cause the fog to deepen more rapidly, with a deep, relatively well mixed fog layer forming capped by an inversion.

- The reason for this early deepening and lifting has not been investigated. Possible factors include

a) Too strong a mean flow, leading to excessive vertical turbulent mixing.

b) Incorrect turbulent transfer coefficients (due to stability functions, mixing lengths etc.) leading to excessive vertical turbulent mixing.
c) Incorrect mixing (vertical and horizontal) due to numerical inaccuracies.
d) Incorrect cloud top entrainment parametrization.
e) Incorrect radiative cooling profile, due to incorrect moisture (liquid and vapour) or temperature profiles, incorrect surface temperature or errors in the radiation scheme.

The large scale pressure field suggests that a) is unlikely, but, with such light winds the possibility should not be entirely discounted. Problems with the turbulent transfer scheme may well exist (see, for example, Dunlop, 1998), but this, in itself, does not explain the sensitivity to horizontal resolution. The fact that higher vertical resolution produces a stronger response suggests that the problem is not simply related to poor vertical resolution. The higher vertical resolution runs do produce initially shallow, thicker fog with a lower surface temperature and stronger surface inversion as, we believe, is required; only in the higher horizontal resolution runs does this grow beyond the depth of the lower vertical resolution runs. A level sensitivity in the boundary layer scheme is a possibility, but it is also possible that the boundary layer scheme, at higher vertical resolution, is responding correctly to stronger cloud top cooling. The thicker fog may lead to earlier onset of convective instability at the fog top. In the higher horizontal resolution runs, the forcing (through surface slope) is larger, leading to an additional surface cooling over a given area, while the horizontal diffusive coupling (through both actual and numerical diffusion) is less. This may account for the generally stronger winds

If the fog is, indeed, excessively deep it would be expected to be more affected by the mean geostrophic flow and be transported more strongly. There is a suggestion, however, that the low level winds are themselves too strong. The SW wind near the surface up the Severn valley is curious; it follows the geostrophic wind direction quite well but does not seem to verify well. This suggests that the vertical temperature gradient near the surface is insufficient to produce an opposing (down-slope) pressure gradient along the valley floor, compared with the synoptic scale gradient, though the valley sides are, indeed, steep enough to strongly divert the flow.

The higher resolution models (both vertically and horizontally) show elevated inversions as early as 18Z. Error may be inherited from initial conditions; the synoptic conditions were extremely static, and the initial field was remarkably similar to the T+24 12 k m UM, i.e. with deep stratocumulus over the main valleys. Thus, it is possible that radiative cooling was at too high a level from the outset. Again, this does not explain the resolution dependence. Since the behaviour itself (i.e. becoming convectively mixed and lifting) is observed in other cases, and is not unphysical, it is conceivable that the higher resolution model is responding accurately to incorrect forcing from incorrect initial conditions, while the lower resolution model is not.

4 Conclusions and Recommendations

1. In this case, the forecast of fog shows strong sensitivity to the choice of physics and/or sub-surface conditions. This sensitivity appears to be at least as great as sensitivity to dynamics.

2. The ND at operational resolution performs generally better objectively and subjectively than the hydrostatic UM with the same physics.

3. Comparison between UM and ND is scientifically compromised by the difficulty of tracing the exact physics formulation used in each model.

4. Sensitivity to vertical resolution is not strong at operational (12 km) resolution.

5. The ND has been successfully run at 4 km and 2 km resolution. Both produce very good short (6-12h) forecasts compared with the 12 km model, though the benefit of going from 4 to 2 km is not clear.

6. A 12 h forecast covering the whole UK at 4 km would be a practical proposition, given the additional computing power required to add this to our current operational suite.

7. Higher resolution runs exhibit problems with excessive deepening and thickening as time progresses, and eventually perform worse than lower resolution runs. The reason for this behaviour is unknown, but possible explanations include inaccurate initial conditions or excessive entrainment through the fog top in the boundary layer scheme.

8. The reasons for the model behaviour have not been investigated in depth because the model physics is regarded as volatile in the UM at present; a similar exercise should be repeated with a more stable and well documented physics version (i.e. UM version 5.2+) and VAR data assimilation, at least in the 12 km run, with reconfiguration from ND grid to ND grid.

9. In a repeat exercise, attention should be addressed to surface exchange, cloud top entrainment and radiative cooling processes in particular.

5 References

Clark, P.A., Hopwood, W. P., Best, M. J. Dunlop, C. C. and Maisey, P. E., 1997, Assessment of the first version of the Site Specific Forecast Model, NWP Technical Report No. 213.

Dunlop, C.C., 1998, Stable boundary layers: sensitivity to stability functions and comparison with observations, NWP Technical Report No. 240.

CURRENT JCMM INTERNAL REPORTS

This series of JCMM Internal Reports, initiated in 1993, contains unpublished reports and also versions of articles submitted for publication. The complete set of Internal Reports is available from the National Meteorological Library on loan, if required.

1. **Research strategy and programme**
   K A Browning et al
   January 1993

2. **The GEWEX Cloud System Study (GCSS)**
   GEWEX Cloud System Science Team
   January 1993

3. **Evolution of a mesoscale upper tropospheric vorticity maximum and comma cloud from a cloud-free two dimensional potential vorticity anomaly**
   K A Browning
   January 1993

4. **The global energy and water cycle**
   K A Browning
   July 1993

5. **Structure of a midlatitude cyclone before occlusion**
   K A Browning and N Roberts
   July 1993

6. **Developments in systems and tools for weather forecasting**
   K A Browning and G Szejwach
   July 1993

7. **Diagnostic study of a narrow cold frontal rainband and severe winds associated with a stratospheric intrusion**
   K A Browning and R Reynolds
   August 1993

8. **Survey of perceived priority issues in the parametrizations of cloud-related processes in GCMs**
   K A Browning
   September 1993

9. **The effect of rain on longwave radiation**
   I Dharssi
   September 1993

10. **Cloud microphysical processes - a description of the parametrization used in the large eddy model**
    H Swann
    October 1993

11. **An appreciation of the meteorological research of Ernst Kleinschmidt**
    A J Thorpe
    May 1992

12. **Potential vorticity of flow along the Alps**
    A J Thorpe, H Volkert and Dietrich Heimann
    August 1992

13. **The representation of fronts**
    A J Thorpe
    January 1993

14. **A parametrization scheme for symmetric instability: test for an idealised flow**
C S Chan and A J Thorpe
February 1993

15. **The Fronts 92 Experiment: a Quicklook Atlas**
Edited by T D Hewson
November 1993

16. **Frontal wave stability during moist deformation frontogenesis**
Part 1: Linear wave dynamics
C H Bishop and A J Thorpe
May 1993

17. **Frontal wave stability during moist deformation frontogenesis**
Part 2. The suppression of non-linear wave development
C H Bishop and A J Thorpe
May 1993

18. **Gravity waves in sheared ducts**
S Monserrat and A J Thorpe
October 1993

19. **Potential vorticity and the electrostatics analogy: quasi-geostrophic theory**
C Bishop and A J Thorpe
November 1993

20. **Recent advances in the measurement of precipitation by radar**
A J Illingworth
April 1993

21. **Micro-physique et givrage: cloud microphysics and aircraft icing**
A J Illingworth
May 1993

22. **Differential phase measurements of precipitation**
M Blackman and A J Illingworth
May 1993

23. **Estimation of effective radius of cloud particles from the radar reflectivity**
N I Fox and A J Illingworth
May 1993

24. **A simple method of Dopplerising a pulsed magnetron radar**
A Hua, A J Illingworth and J Eastment
November 1993

25. **Radiation and polar lows**
George C Craig
February 1994

26. **Collected preprints submitted to the International Symposium on the Life Cycles of Extratropical Cyclones; Bergen, Norway, 27 June - 1 July 1994**
April 1994

27. **Convective frontogenesis**
Douglas J Parker and Alan J Thorpe
April 1994

28. **Improved measurement of the ice water content in cirrus using a total water evaporator**
Philip R A Brown and Peter N Francis
April 1994

29. **Mesoscale effects of a dry intrusion within a vigorous cyclone**
K A Browning and B W Golding
April 1994

30. **GEWEX Cloud System Study, Science Plan**
May 1994

31. **Parametrization of momentum transport by convectively generated gravity waves**
R Kershaw
May 1994

32. **Mesoscale Modelling Newsletter No 5**
May 1994

33. **Observations of the mesoscale sub-structure in the cold air of a developing frontal cyclone**
K A Browning, S A Clough, C S A Davitt, N M Roberts and T D Hewson
May 1994

34. **Longwave radiative forcing of a simulated tropical squall line**
Imtiaz Dharssi
July 1994

35. **On the nature of the convective circulation at a kata-cold front**
K A Browning
September 1994

36. **Collective preprints of papers submitted to the COST-75 International Seminar on Advanced Weather Radar Systems, Brussels, 20-23 September 1994**
November 1994

37. **Use of satellite imagery to diagnose events leading to frontal thunderstorms: Parts I and II of a case study**
K A Browning and N M Roberts
November 1994

38. **The role of spaceborne millimetre-wave radar in the global monitoring of ice cloud**
P R A Brown, A J Illingworth, A J Heymsfield, G M McFarquhar, K A Browning and M Gosset
December 1994

39. **Potential vorticity inversion**
Michal Ziemianski
October 1994

40. **Theory of mature tropical cyclones; a comparison between Kleinschmidt (1951) and Emanuel (1986)**
Suzanne L Gray
December 1994

41. **Dispersion and removal of pollutants during the passage of an atmospheric frontal system**
N R Gimson
December 1994

42. **The role of snow sublimation in frontogenesis**
D J Parker and A J Thorpe
December 1994

43. **Potential vorticity and the electrostatics Analogy: Ertel-Rossby formulation**
A J Thorpe and C H Bishop
December 1994

44. **Mesoscale aspect of extratropical cyclones: an observational perspective**
K A Browning
January 1995

45. **A polar low outbreak: evolution and mesoscale structures**
T D Hewson, G C Craig and C Claud
February 1995

46. **Generation of near-surface gusts of deep convection**
K Nakamura and R Kershaw
April 1995

47. **Attribution concepts applied to the Omega Equation**
S A Clough, C S A Davitt and A J Thorpe
June 1995

48. **Parametrization of mixed-phase cloud and precipitation**
Susan P Ballard and M Gerard Hutchinson
June 1995

49. **Short-range forecasting of stratocumulus: initialization prediction**
Susan P Ballard, Simon D Jackson and B Macpherson
June 1995

50. **Contributions of the JCMM/Dept of Meteorology Radar Group to the 27th AMS Radar Meteorology Conference, Vail October 1995**
June 1995

51. **Cold pools in shear**
Douglas J Parker
September 1995

52. **High-resolution analysis of frontal fracture**
K A Browning, S P Ballard and C S A Davitt
September 1995

53. **The albedo of broken cloud fields: calculations using a modified two stream radiation code**
Imtiaz Dharssi and Roy Kershaw
October 1995

54. **Parametrization of momentum transport by convection. I: theory and cloud modelling results**
R Kershaw and D Gregory
November 1995

55. **Variation of frontal structure along a cold front**
K A Browning and N M Roberts
November 1995

56. **Secondary frontal waves**
Douglas Parker
December 1995

57. **Objective fronts**
T D Hewson
March 1996

58. **Mesoscale analysis of the activation of a cold front during cyclogenesis**
K A Browning, N M Roberts and A J Illingworth
June 1996

59. **Investigation of different representations of rain in a 1-d evaporation model**
H Swann
May 1996

60. **Parametrization of diabatic processes in the inversion of the omega-equation**
M Athanassiadou and A J Thorpe
June 1996

61. **The role of the environmental flow in the development of secondary frontal cyclones**
I A Renfrew, A J Thorpe and A Joly
June 1996

62. **Consequences of the geostrophic momentum approximation on barotropic instability**
S Malardel, A J Thorpe and A Joly
June 1996

63. **Contributions to the AMS/RMS Conference on Mesoscale Processes**
Reading, 9-13 September 1996

64. **Vorticity and potential vorticity in stratified flows interacting with an isolated obstacle**
Jorge A Gutiérrez and A J Thorpe
September 1996

65. **Triple point development: two case studies**
Douglas Parker
September 1996

66. **Radar observations of wind-shear splitting within evolving atmospheric Kelvin-Helmholtz billows**
D Chapman and K A Browning
April 1997

67. **Cold frontal structure derived from radar wind profilers**
K A Browning, D Jerrett, J Nash, T Oakley and N M Roberts
May 1997

68. **The dry intrusion and its effect on the frontal, cloud and precipitation structure of extratropical cyclones**
K A Browning - Text of invited special lecture at the Spring Conference
of the Meteorological Society of Japan, University of Tsukuba, 22 May 1997

69. **Met. Office Unified Model data, diagnostics, graphics programs, and other observational data available from the JCMM through the aegis of the Universities Weather Research Network (UWERN).** (Plus supplement)
Peter Panagi and Ed Dicks
June 1997

70. **Contributions of the JCMM/Dept of Meteorology Radar Group to the 28th AMS Radar Meteorology Conference.** Austin, Texas
September 1997

71. **Sensitivity of short-range weather forecasts to local potential vorticity modifications**
Meral Demirtas and Alan Thorpe
July 1997

72. **Objective identification of frontal wave cyclones**
T D Hewson
August 1997

73. **Attribution and its application to mesoscale structure associated with tropopause folds**
A J Thorpe
September 1997

74. **The role of the environmental flow in the development of secondary frontal cyclones**
Ian A Renfrew, Alan J Thorpe and Craig H Bishop
September 1997

75. **Potential vorticity: a short history of its definitions and uses**
Alan J Thorpe and Hans Volkert
September 1997

76. **Superposing semi-geostrophic potential vorticity anomalies**
H R Birkett and A J Thorpe
September 1997

77. **Short period forecasting of catchment-scale precipitation.**
Part 1: the role of Numerical Weather Prediction
M A Pedder, M Haile and A J Thorpe
September 1997

78. **Verification of the tracking technique used in an experimental cloud motion wind inferring system**
Z Wang, K A Browning and G A Kelly
October 1997

79. **A preliminary study of Fourier series analysis for cloud tracking with GOES high temporal resolution images**
Z Wang
October 1997

80. **Analysis of an ex-tropical cyclone after reintensifying as a warm-core extratropical cyclone**
K A Browning, G Vaughan and P Panagi
November 1997

81. **A JCMM overview of FASTEX IOPs**
S A Clough, H W Lean, N M Roberts, H Birkett, J-P Chaboureau, R Dixon, M Griffiths, T D Hewson and A Montani
January 1998

82. **Programs for PV inversion and modification**
Meral Demirtas
December 1997

83. **Release of potential shearing instability in warm frontal zones**
D Chapman and K A Browning
February 1998

84. **The European Cloud-Resolving Modelling Programme (EUCREM)**
Summary Report from the coordinator
P W White
April 1998

85. **A frontal wave database**
T D Hewson
April 1998

86. **Layering observed in dropsoundings from IOP 1 of Fronts 92**
S A Clough
May 1998

87. **Use of wind-shear displays for Doppler radar data**
D Chapman and K A Browning
May 1998

88. **Radar estimates of rainfall rates at the ground in bright band and non-bright band events**
T J Smyth and A J Illingworth
June 1998

89. **Correction for attenuation of radar reflectivity using polarisation data**
T J Smyth and A J Illingworth
June 1998

90. **The effects of convection on chemical reactions and precipitation scavenging**
Neil R Gimson
July 1998

91. **How to use the display program DISP**
Nigel Roberts
August 1998

92. **Conceptual models of cyclogenesis**
Adrian T Semple
August 1998

93. **Observations of oblate hail using dual polarisation radar and implications for hail detection schemes**
T J Smyth, T M Blackman and A J Illingworth
September 1998

94. **The semigeostrophic diagnosis of vertical motion. Part I: Formulation and co-ordinate transformations**
Mike A Pedder and Alan J Thorpe
September 1998

95. **The semigeostrophic diagnosis of vertical motion. Part II: Results for an idealised baroclinic wave life cycle**
Alan J Thorpe and Mike A Pedder
September 1998

96. **Convective destabilisation by a tropopause fold diagnosed using potential vorticity inversion**
Morwenna Griffiths, Alan Thorpe and Keith Browning
October 1998

97. **Forecast skill of the ECMWF model using targeted observations during FASTEX**
A Montani, A J Thorpe, R Buizza and P Unden
October 1998

98. **Observations and model simulations of the FASTEX IOP 16 frontal wave - effects of sublimation**
Sid A Clough, Humphrey W Lean, Nigel M Roberts and Richard M Forbes
December 1998

99. **The application of conceptual models in NWP**
Adrian T Semple
January 1999

100. **Mesoscale analysis of arc rainbands in a dry slot**
K A Browning and N M Roberts
January 1999

101. **Interaction of mesoscale tropopause depressions with a warm-core cyclone: observational and model analyses, and sensitivity to analysis errors**
K A Browning, A J Thorpe, A Montani, D Parsons, M Griffiths, P Panagi and E M Dicks
February 1999

102. **The use of water vapour imagery and PV inversion to adjust initial conditions in NWP**
Sean J Swarbrick
February 1999
This report is no longer available; see Internal Report No.108

103. **Summary notes for a lecture course on Waves in the Atmosphere and Ocean**
A A White
March 1999

104. **Results of a questionnaire on the operational value of conceptual models (CMs) of fronts and cyclones**
N M Roberts & M V Young
July 1999

105. **Contributions to the Poster Session at the 1998 UWERN Annual Science Meeting**
assembled by A A White
August 1999

106. **The objective analysis of dropsonde data from FASTEX**
Richard Forbes, Sid Clough, Mark Dixon, Andy Macallan & Nigel Roberts
January 2000

107. *NWP Technical Report No.302*
Implications for Mesoscale Modelling from a Study of the FASTEX IOP 16 Mid-latitude Cyclone
Richard M Forbes, Humphrey W Lean, Nigel M Roberts and Peter A Clark
March 2000

108. *NWP Technical Report No.291*
The use of water vapour imagery and PV inversion to adjust initial conditions in NWP
Final Project Report
Sean J Swarbrick
September 1999

109. *NWP Technical Report No.294*
A guide to aspects of water vapour imagery interpretation: the significance of dry regions
Nigel M Roberts
January 2000

110. *NWP Technical Report No.300*
The relationship between water vapour imagery and thunderstorms
Nigel M Roberts
February 2000

111. *NWP Technical Report No.293*
Holomorphic structures in hydrodynamical models of nearly geostrophic flow
V N Roubtsov and I Roulstone
January 2000

112. *NWP Technical Report No.301*
Multi-sensor synthesis of the mesoscale structure of a cold-air comma cloud system
K A Browning, P Panagi and E M Dicks
March 2000

113. *NWP Technical Report No.307*
Observations of stratospheric air entering the circulation of a polar low
K A Browning and E M Dicks
May 2000

114. *NWP Technical Report No.309*
Wind profiler – Unified Model comparison statistics
Peter Panagi & Ed Dicks
March 2000

115. *NWP Technical Report No.310*
Towards a similarity theory of moist convective updrafts
Olaf Stiller and George C Craig
May 2000

116. *NWP Technical Report No.312*
The mystery of striated cloud heads in satellite imagery
R S Dixon, K A Browning and G J Shutts
April 2000

117. *NWP Technical Report No.313*
MDIAG: a Fortran 90 program to compute diagnostics on pressure levels from Unified Model data on model levels
Peter Panagi
June 2000

118. *NWP Scientific Paper No.56*
Rearrangements of functions with applications to meteorology and ideal fluid flow
R J Douglas
June 2000

119. *NWP Technical Report No.320*
Tests of New Dynamics Model on the FASTEX IOP16 case
Humphrey Lean
September 2000

120. *NWP Scientific Paper 57*
A classification of FASTEX cyclones using a height-attributable QG vertical motion diagnostic
A C L Deveson, K A Browning, T D Hewson
September 2000

121. *NWP Scientific Paper 59*
Measurements of dissipation rate in frontal zones
D.Chapman, K A Browning
August 2000

122. *NWP Technical Report 331*
Not Issued yet

123. *NWP Technical Report 337*
A Case Study of High Resolution Fog Forecasts with the New Dynamics
P. Clark
November 2000

Met Office Joint Centre for Mesoscale Meteorology Department of Meteorology
University of Reading PO Box 243 Reading RG6 6BB United Kingdom
Tel: +44 (0)118 931 8425 Fax: +44 (0)118 931 8791
www.metoffice.com